Contemporary Mathematics
http://ojs.wiserpub.com/index.php/CM/

Research Article

Fractional Dynamics of Nonlinear Kersten-Krasil'shchik Coupled KdV-mKdV Systems: Analytical Insights Through Analytical Methods

Yousuf Alkhezi[1], Ahmad Shafee[2*]

[1] Mathematics Department, College of Basic Education, Public Authority for Applied Education and Training (PAAET), Shuwaikh 70654, Kuwait
[2] Laboratory Technology Department, College of Technological Studies, Public Authority for Applied Education and Training (PAAET), Shuwaikh 70654, Kuwait
E-mail: as.zada@paaet.edu.kw

Received: 25 January 2026; **Revised:** 30 March 2026; **Accepted:** 24 April 2026

Abstract: This study examines the fractional order formulations of the nonlinear coupled Korteweg-de Vries type systems in the wave interaction phenomena, especially the Kersten-Krasil'shchik KdV-mKdV system and a two-component coupled KdV model. The ϕ-Caputo fractional derivative is used to describe the time evolution of the systems and offers a versatile framework for integrating memory and nonlocal time effects. Two effective semi-analytical methods, the ϕ-Caputo fractional q-homotopy analysis method, and the ϕ-Caputo fractional variational iteration method, are proposed to derive analytical approximations. Clear series solutions are developed and demonstrated to converge very fast when appropriate auxiliary parameters are chosen. The effect of the fractional order on the dynamical behavior of the solutions is explored in detail using two and three dimensional graphs. It has been shown that as the fractional order is lowered the wave profile becomes smoother with a reduction in amplitude, which reflects an increase in the effect of memory. The close similarity of the approximate solutions obtained and the exact solutions in the case of integer-order validates the precision and accuracy of the proposed methods. The fractional models in this paper provide a better understanding of the nonlinear propagation of waves in complex media where classical integer-order models might fail.

Keywords: ϕ-Caputo fractional operator, fractional-order partial differential equations, nonlinear Kersten-Krasil'shchik coupled KdV-mKdV systems, q-homotopy analysis method, variational iteration method (VIM)

MSC: 26A33, 35R11, 35Q53, 65M99, 65H20

1. Introduction

Fractional calculus (FC) provides a rigorous mathematical framework for modeling complex systems with memory and nonlocal effects, enabling a more accurate description of real-world phenomena. Another layer for better understanding or expressing fundamental natures is provided by making this subject available to the scientific and technical communities as a global topic. This is an efficient way to communicate with nature since FC is the language that it understands. For the last three centuries, mathematicians have dealt with this FC problem; more lately, it has been incorporated into other useful fields of science, engineering, and economics [1–6]. Integrals and derivatives in any real or complex order are

Copyright ©2026 Yousuf Alkhezi, et al.
DOI: https://doi.org/10.37256/cm.7420269668
This is an open-access article distributed under a CC BY license
(Creative Commons Attribution 4.0 International License)
https://creativecommons.org/licenses/by/4.0/

handled by FC. In order to handle practical applications, several fractional operators have lately been proposed and put into practice. Using the ϕ-Caputo, we examined a generalized fractional operator in this study that may be utilized to simulate a number of real-world problems. It has been referred to because of its generalizability to other fractional operators, and there are several example applications in the literature [7–11]. The fractional operational matrix methodology [12], Shehu decomposition technique [13, 14], q-homotopy transformation method [15], homotopy perturbation method [16, 17], and variational iteration transform technique [18] are some of the main tactics that have been used.

A significant category of mathematical models that describe complex systems is now nonlinear fractional-order partial differential equations (NFPDEs), as classical integer-order equations are no longer sufficient because of memory and nonlocal effects [19]. These equations can exhibit anomalous diffusion, viscoelastic behavior and wave propagation in heterogeneous and complex media much better through the use of fractional derivatives [20, 21]. With the addition of nonlinear terms, the fractional-order models can describe some of the most important physical processes, including the interaction of solitons, the formation of shocks, and the mechanisms of energy exchange [22]. The most notable nonlinear equations, such as fractional Korteweg-de Vries (KdV), Burgers, Navier-Stokes, and nonlinear Schrödinger equations, have received intensive research over the past few years [23]. Nonlinearity, however, is very strong in combination with the presence of the fractional operators, making the analysis of the solutions to be very challenging; this has led to the development of effective analytical and semi-analytical methods of finding solutions including the homotopy analysis method, variational iteration method, and decomposition based methods [22, 23]. Therefore, nonlinear fractional-order partial differential equations still receive significant interest because of their high level of theoretical significance and broad usage in science and engineering [20, 24].

There are many uses for the KdV type of equations in the engineering and physical sciences, making it a significant class of non-linear evolution equations. For instance, they describe a long wave in deep oceans and shallow seas in geophysical fluid dynamics [25, 26]. The ion acoustic solutions in plasma physics are derived from these equations [27–29]. However, because constant coefficients are assumed, the practical scenarios in which the KdV equations appear are often extremely oversimplified. Many writers have focused on studying coupled equation solutions using a variety of techniques in recent years. These include the F-expansion transform technique [30], the homogeneous balance method [31], the trigonometric function transform method [32], the homotopy perturbation method [33], and the He's variational iteration approach [34].

Due to its potential applications in fluid dynamics, nonlinear optics, and plasma physics, Kersten-Krasil'shchik coupled Korteweg-de Vries (KdV)-modified KdV (mKdV) systems have been the subject of much recent study [35–38]. Fractional derivatives, which add non-local and memory effects to the system's dynamics, are a defining feature of these systems [39–42]. Two linked nonlinear partial differential equations that explain the development of two waves in a dispersive medium make up the Kersten-Krasil'shchik coupled KdV-mKdV system. The first is the well-known KdV equation, which governs the propagation of long-wavelength, small-amplitude waves. The propagation of waves with shorter wavelengths and greater amplitudes is described by the second equation, the mKdV equation. The two waves' interaction is described by the nonlinear and non-local Kersten-Krasil'shchik coupling factor [43–45]. In 2018, Li et al. investigated the study of an epidemic model and its comparisons with other processes [46], while in 2016, Jin and Wang investigated the phenomenon of chemotaxis [47]. He et al. [48] first addressed fixed-point and variational inequality problems for Hadamard manifolds in 2022 , and then in 2023 [49] they talked about nonexpansive mapping techniques. By identifying hidden-charm pentaquarks in 2021, Chen et al. [50] made a contribution to particle physics. In 2023, Yang and Kai studied nonlinear Schroder equations, while Lyu et al. examined cavity dynamics in water entry [51].

The recent progress in approximation theory and operator-based analytical models have contributed greatly to the analysis of nonlinear dynamical systems. Specifically, wavelet-based methods and the operators of q-calculus stimulations have become one of the potent approaches to enhance the quality of approximation and study the convergence. The construction of blending-type q-Baskakov operators together with wavelet transformations, which provide a rigorous framework for approximation and convergence, serves as a pertinent example and is directly applicable to the validation of the rapidly convergent series solutions produced by semi-analytical methods [52]. Likewise, quadratic function retaining wavelet-type Baskakov operators have been suggested to improve the functional approximation, and prove the efficiency of specialized operators in the representation of sophisticated nonlinear processes [53].

Additionally, the recent advances of operator-based interpolation techniques have created the modern views of the computation into classical analysis. The neural network-based operators on complex domains to interpolate boundaries provide an efficient and flexible alternative to the classical analytical schemes, and such innovations can be considered complemented with the iterative methods, such as the variational iteration method that was used in this work [54]. Moreover, the development of ǵ-statistical approximation with wavelet-based Kantorovich-typeǵ-Baskakov operators offers an excellent theoretical basis of analytical procedures, thus contributing to the development of the q-homotopy analysis method adopted in this research paper [55].

Also, the combination of superior techniques of approximation with realistic physical models has received much attention. The use of deep neural network architectures to the complex fluid flow and heat transfer systems demonstrates the rising tendency of integrating both the analytical and data-driven approaches to the solution of nonlinear systems [56]. All these developments underline the need to have strong, precise and convergent solution methods to nonlinear differential equations.

Inspired by these developments, this paper uses effective semi-analytical methods, the ϕ-Caputo homotopy analysis method (ϕ_C-qHAM) and the ϕ-Caputo variational iteration method (ϕ_C-VIM) in the framework of the ϕ-Caputo fractional calculus to obtain the accurate and fast converging analytical approximations to the nonlinear coupled KdV equations and the coupled Kersten-Krasil'shchik KdV-mKdV equations. The suggested method not only guarantees the optimal level of accuracy and speed of convergence, but also serves the further goal of creating effective instruments of analysis of the nonlinear wave propagation in the complex media with the significant influence of memory and nonlocal effects.

2. Preliminaries

This section summarizes the essential notions of fractional calculus required throughout the analysis.

Definition 1 [57, 58] Let Θ be the function of spatial variable τ and temporal variable υ, defined on the interval $I=[d_1,d_2]$ with respect to ϕ of order δ, where $\phi\in C^1(I)$ is strictly increasing, $\phi'(\upsilon)\neq 0$ for every $\upsilon\in I$, and $\delta>0$. The left-sided fractional integral of Θ is introduced by

$$\mathscr{J}_{d_1}^{\delta;\phi}[\Theta(\tau,\upsilon)]=\frac{1}{\Gamma(\delta)}\int_{d_1}^{\upsilon}\phi'(\rho)\,(\phi(\upsilon)-\phi(\rho))^{\delta-1}\,\Theta(\tau,\rho)\,d\rho. \tag{1}$$

For the case $\delta=0$, the operator reduces to

$$\mathscr{J}_{d_1}^{0;\phi}[\Theta(\tau,\upsilon)]=\Theta(\tau,\upsilon). \tag{2}$$

Theorem 1 [58] Consider $\delta>0$, $s\in\mathbb{N}$, and $\Theta,\phi\in C^s(I)$ where $I=[d_1,d_2]$, with ϕ strictly increasing and satisfying $\phi'(\upsilon)\neq 0$ on I. The left-sided ϕ–Caputo fractional derivative of order δ is defined by

$${}^{\mathscr{C}}_{d_1}\mathscr{D}_{\upsilon}^{\delta;\phi}[\Theta(\tau,\upsilon)]=\mathscr{J}_{d_1}^{s-\delta;\phi}\left(\frac{1}{\phi'(\upsilon)}\frac{\partial}{\partial\upsilon}\right)^{s}\Theta(\tau,\upsilon), \tag{3}$$

where $s=[\delta]+1$ for non-integer δ and $s=\delta$ when $\delta\in\mathbb{N}$.

A compact representation of the higher-order ϕ-derivative is

$$\Theta^{[s];\phi}(\tau,\upsilon)=\left(\frac{1}{\phi'(\upsilon)}\frac{\partial}{\partial\upsilon}\right)^{s}\Theta(\tau,\upsilon). \tag{4}$$

As noted in [59], the classical Caputo operator is recovered when $\phi(\mho) = \mho$, while choosing $\phi(\mho) = \ln(\mho)$ yields the Caputo-Hadamard operator [60].

Theorem 2 [60] Let $\Re(\delta) \geq 0$ and define $s = [\Re(\delta)] + 1$. If $\Theta \in C^s_\lambda([\varsigma_1, \varsigma_2])$ for $0 < \varsigma_1 < \varsigma_2 < \infty$ and

$$AC^s_\lambda([\varsigma_1, \varsigma_2]) = \left\{ g : [\varsigma_1, \varsigma_2] \to \mathbb{C} \ : \ \lambda^{s-1} g(\tau) \in AC[\varsigma_1, \varsigma_2],\ \lambda = \tau \frac{d}{d\tau} \right\}, \tag{5}$$

then the Caputo-Hadamard derivative ${}^{\mathscr{C}}_{\varsigma_1}\mathscr{D}^{\delta;\ln(\mho)}_{\mho}\Theta(\mho)$ exists on $[\varsigma_1, \varsigma_2]$ and can be expressed as

$${}^{\mathscr{C}\mathscr{H}}_{\varsigma_1}\mathscr{D}^{\delta}_{\mho}\Theta(\mho) = \frac{1}{\Gamma(s-\delta)} \int_{\varsigma_1}^{\mho} \left(\ln \frac{\mho}{\upsilon} \right)^{s-\delta-1} \left(\mho \frac{d}{d\mho} \right)^{s} \Theta(\upsilon) \frac{d\upsilon}{\upsilon}. \tag{6}$$

Lemma 1 [60] For $\Theta \in AC^s_\lambda([\varsigma_1, \varsigma_2])$ and $\delta \in \mathbb{C}$,

$$\mathscr{J}^{\delta;\ln(\mho)}_{\varsigma_1} \left({}^{\mathscr{C}\mathscr{H}}_{\varsigma_1}\mathscr{D}^{\delta}_{\mho}\Theta(\mho) \right) = \Theta(\mho) - \sum_{k=0}^{s-1} \frac{\lambda^k \Theta(d_1)}{k!} \left(\ln \frac{\mho}{\varsigma_1} \right)^k. \tag{7}$$

Theorem 3 [60] Let $\Theta \in C^s([\varsigma_1, \varsigma_2])$, $s-1 < \delta \leq s$, $s \in \mathbb{N}$, and $\kappa > 0$. Then:
1. If $\Theta(\mho) = (\phi(\mho) - \phi(\vartheta))^{\kappa-1}$,

$$\mathscr{J}^{\delta;\phi}_{\vartheta}[\Theta(\mho)] = \frac{\Gamma(\delta)}{\Gamma(\delta+\kappa)} (\phi(\mho) - \phi(\vartheta))^{\delta+\kappa-1}. \tag{8}$$

2. The composition rule

$$\mathscr{J}^{\delta;\phi}_{\vartheta} \left({}^{\mathscr{C}}_{\vartheta}\mathscr{D}^{\delta;\phi}_{\mho}[\Theta(\tau, \mho)] \right) = \Theta(\tau, \mho) - \sum_{k=0}^{s-1} \frac{\Theta^{[k];\phi}(\tau, \vartheta)}{k!} (\phi(\mho) - \phi(\vartheta))^k \tag{9}$$

holds for all $\mho$ in the domain.

3. Methodology

The section includes the mathematical framework and solution strategies that were used to address the proposed fractional nonlinear coupled KdV-type systems. The governing equations are first developed with the help of the ϕ-Caputo fractional derivative that helps to introduce the concept of memory and the nonlocal effects. Then, two effective semi-analytical methods, the ϕ_C-qHAM and the ϕ_C-VIM, are developed and applied systematically to derive approximate analytical solutions. The convergence property of the solution series that are obtained is also addressed, as well as the use of auxiliary parameters to achieve rapid convergence and accuracy of the solution.

3.1 *The ϕ_C-qHAM*

Here, we summarize the concept of the proposed method for a system of nonlinear fractional partial differential equations. Consider the following coupled system:

$$\begin{cases} \mathcal{N}_1\left(D_{\mho}^{\delta;\phi}\wp_1(\tau,\mho)\right) - f_1(\tau,\mho) = 0, \\ \mathcal{N}_2\left(D_{\mho}^{\delta;\phi}\wp_2(\tau,\mho)\right) - f_2(\tau,\mho) = 0, \end{cases} \tag{10}$$

where $D_{\mho}^{\delta;\phi}$ denotes the ϕ-Caputo fractional derivative, $\mathcal{N}_1$ and $\mathcal{N}_2$ are nonlinear operators, $f_1(\tau,\mho)$ and $f_2(\tau,\mho)$ are known source functions, and $\wp_1(\tau,\mho)$ and $\wp_2(\tau,\mho)$ are the unknown functions of the spatial variable τ and temporal variable $\mho$.

To construct the homotopy framework, the zeroth-order deformation equations are defined as

$$\begin{aligned} &(1-qn)\mathcal{L}(\Phi_1(\tau,\mho;q) - \wp_{1,0}(\tau,\mho)) = hq\,\mathcal{H}(\tau,\mho)\left(\mathcal{N}_1\left[D_{\mho}^{\delta;\phi}\Phi_1(\tau,\mho;q)\right] - f_1(\tau,\mho)\right), \\ &(1-qn)\mathcal{L}(\Phi_2(\tau,\mho;q) - \wp_{2,0}(\tau,\mho)) = hq\,\mathcal{H}(\tau,\mho)\left(\mathcal{N}_2\left[D_{\mho}^{\delta;\phi}\Phi_2(\tau,\mho;q)\right] - f_2(\tau,\mho)\right), \end{aligned} \quad 0 \le q \le \frac{1}{n},\ n \ge 1. \tag{11}$$

Here, q is the embedding parameter, $h\,(h \neq 0)$ is an auxiliary parameter, $\mathcal{L}$ is a linear operator, and $\mathcal{H}(\tau,\mho) \neq 0$ is an auxiliary function. From the above equations, for $q = 0$ and $q = \frac{1}{n}$, we obtain

$$\wp_{1,0}(\tau,\mho) = \Phi_1(\tau,\mho;0), \qquad \wp_1(\tau,\mho) = \Phi_1\left(\tau,\mho;\frac{1}{n}\right), \tag{12}$$

$$\wp_{2,0}(\tau,\mho) = \Phi_2(\tau,\mho;0), \qquad \wp_2(\tau,\mho) = \Phi_2\left(\tau,\mho;\frac{1}{n}\right). \tag{13}$$

As q varies from 0 to $\frac{1}{n}$, the functions $\Phi_1(\tau,\mho;q)$ and $\Phi_2(\tau,\mho;q)$ continuously deform from the initial guesses $\wp_{1,0}(\tau,\mho)$ and $\wp_{1,0}(\tau,\mho)$ to the exact solutions $\wp_1(\tau,\mho)$ and $\wp_2(\tau,\mho)$.

Each embedding function admits the Taylor series expansion

$$\Phi_1(\tau,\mho;q) = \wp_{1,0}(\tau,\mho) + \sum_{r=1}^{\infty}\wp_{1,r}(\tau,\mho)\,q^r, \tag{14}$$

$$\Phi_2(\tau,\mho;q) = \wp_{2,0}(\tau,\mho) + \sum_{r=1}^{\infty}\wp_{2,r}(\tau,\mho)\,q^r, \tag{15}$$

where

$$\wp_{1,r}(\tau,\mho) = \frac{1}{r!}\left.\frac{\partial^r\Phi_1(\tau,\mho;q)}{\partial q^r}\right|_{q=0}, \tag{16}$$

$$\wp_{2,r}(\tau,\mho) = \frac{1}{r!}\left.\frac{\partial^r\Phi_2(\tau,\mho;q)}{\partial q^r}\right|_{q=0}. \tag{17}$$

If convergence is ensured at $q = \frac{1}{n}$, the solutions of the coupled system are expressed as

$$\wp_1(\tau,\mho) = \wp_{1,0}(\tau,\mho) + \sum_{r=1}^{\infty} \wp_{1,r}(\tau,\mho)\left(\frac{1}{n}\right)^r, \tag{18}$$

$$\wp_2(\tau,\mho) = \wp_{2,0}(\tau,\mho) + \sum_{r=1}^{\infty} \wp_{2,r}(\tau,\mho)\left(\frac{1}{n}\right)^r. \tag{19}$$

Define the solution vectors

$$\vec{\wp}_{1,\omega} = [\wp_{1,0}(\tau,\mho), \wp_{1,1}(\tau,\mho), \ldots, \wp_{1,\omega}(\tau,\mho)], \tag{20}$$

$$\vec{\wp}_{2,\omega} = [\wp_{2,0}(\tau,\mho), \wp_{2,1}(\tau,\mho), \ldots, \wp_{2,\omega}(\tau,\mho)]. \tag{21}$$

By differentiating the zeroth-order deformation equations r times with respect to q, setting $q = 0$, and dividing by $r!$, the r^{th}-order deformation equations are obtained as (Iyiola et al. [61]; Liao [62])

$$\mathscr{L}(\wp_{1,r}(\tau,\mho) - \Psi_r^* \wp_{1,r-1}(\tau,\mho)) = h\mathscr{H}(\tau,\mho)\mathscr{R}_{1,r}(\vec{\wp}_{1,r-1}), \tag{22}$$

$$\mathscr{L}(\wp_{2,r}(\tau,\mho) - \Psi_r^* \wp_{2,r-1}(\tau,\mho)) = h\mathscr{H}(\tau,\mho)\mathscr{R}_{2,r}(\vec{\wp}_{2,r-1}), \tag{23}$$

subject to the initial conditions

$$\wp_{1,r}^{(\varphi)}(\tau,0) = 0, \tag{24}$$

$$\wp_{2,r}^{(\varphi)}(\tau,0) = 0, \qquad \varphi = 0,1,2,\ldots,r-1. \tag{25}$$

Here,

$$\mathscr{R}_{1,r}(\vec{\wp}_{1,r-1}) = \frac{1}{(r-1)!}\frac{\partial^{r-1}}{\partial q^{r-1}}\left(\mathscr{N}_i\left[D_{\mho}^{\delta}\Phi_1(\tau,\mho;q)\right] - f_1(\tau,\mho)\right)\Big|_{q=0}, \tag{26}$$

$$\mathscr{R}_{2,r}(\vec{\wp}_{2,r-1}) = \frac{1}{(r-1)!}\frac{\partial^{r-1}}{\partial q^{r-1}}\left(\mathscr{N}_2\left[D_{\mho}^{\delta}\Phi_2(\tau,\mho;q)\right] - f_2(\tau,\mho)\right)\Big|_{q=0}, \tag{27}$$

and

$$\Psi_r^* = \begin{cases} 0, & r \le 1, \\ n, & r > 1. \end{cases} \tag{28}$$

Note: The auxiliary parameters are selected following the standard convergence-control strategy of the homotopy analysis method (HAM) [24, 62]. For the integer-order case ($\delta = 1,\ \phi(\mho) = \mho$), the linear operator is taken as $\mathscr{L}$ ($n = 1$) because the governing equations are first-order in time, which is the simplest choice that ensures the convergence of the series [24]. The convergence-control parameter h is determined by constructing the h-curve, where the residual error or the value of the solution at a fixed point is plotted against h; the optimal value is chosen from the flat region where the series remains stable [62, 63]. The value $h = -1$ lies in this flat region and, for many nonlinear problems, simplifies the deformation equation to a form that often yields rapid convergence [24, 61]. This selection is further validated by comparing the series with the exact solitary wave solution; with $h = -1$ the series converges to the exact solution with a minimal number of terms, confirming its optimality for the present KdV-type system.

4. The ϕ_C-VIM

In this section, the conformable fractional variational iteration method is extended to the framework of the ϕ–Caputo fractional derivative for solving a coupled system of nonlinear time-fractional partial differential equations. Consider the following system

$$\begin{aligned} &\mathscr{D}_{\mho}^{\delta;\phi} \wp_1(\tau,\mho) + L_1(\wp_1(\tau,\mho), \wp_2(\tau,\mho)) + N_1(\wp_1(\tau,\mho), \wp_2(\tau,\mho)) = h_1(\tau,\mho), \\ &\mathscr{D}_{\mho}^{\delta;\phi} \wp_2(\tau,\mho) + L_2(\wp_1(\tau,\mho), \wp_2(\tau,\mho)) + N_2(\wp_1(\tau,\mho), \wp_2(\tau,\mho)) = h_2(\tau,\mho), \end{aligned} \tag{29}$$

where $\mathscr{D}_{\mho}^{\delta;\phi}$ denotes the left-sided ϕ–Caputo fractional derivative of order $s-1 < \delta \le s$, $s \in \mathbb{N}$, L_1, L_2 and N_1, N_2 represent the linear and nonlinear operators, respectively, and $h_1(\tau,\mho)$ and $h_2(\tau,\mho)$ are known source functions.

Using Definition (3) and the compact notation of the higher-order ϕ-derivative given in (4), the above system can be rewritten as

$$\begin{aligned} &\mathscr{J}_0^{s-\delta;\phi}\left(\wp_1^{[s];\phi}(\tau,\mho)\right) + L_1(\wp_1(\tau,\mho), \wp_2(\tau,\mho)) + N_1(\wp_1(\tau,\mho), \wp_2(\tau,\mho)) = h_1(\tau,\mho), \\ &\mathscr{J}_0^{s-\delta;\phi}\left(\wp_2^{[s];\phi}(\tau,\mho)\right) + L_2(\wp_1(\tau,\mho), \wp_2(\tau,\mho)) + N_2(\wp_1(\tau,\mho), \wp_2(\tau,\mho)) = h_2(\tau,\mho). \end{aligned} \tag{30}$$

According to the variational iteration methodology, the correction functionals for the coupled system are constructed as

$$\begin{aligned}\wp_{1,n+1}(\tau,\upsilon) =& \wp_{1,n}(\tau,\upsilon) + \int_0^{\upsilon} \mu_1(\rho)\Big[\wp_{1,n}^{[s];\phi}(\tau,\rho) + L_1(\wp_{1,n},\wp_{2,n}) \\ &+ N_1(\tilde{\wp}_{1,n},\tilde{\wp}_{2,n}) - h_1(\tau,\rho)\Big]\phi'(\rho)\,d\rho, \\ \wp_{2,n+1}(\tau,\upsilon) =& \wp_{2,n}(\tau,\upsilon) + \int_0^{\upsilon} \mu_2(\rho)\Big[\wp_{2,n}^{[s];\phi}(\tau,\rho) + L_2(\wp_{1,n},\wp_{2,n}) \\ &+ N_2(\tilde{\wp}_{1,n},\tilde{\wp}_{2,n}) - h_2(\tau,\rho)\Big]\phi'(\rho)\,d\rho,\end{aligned} \tag{31}$$

where $\mu_1(\rho)$ and $\mu_2(\rho)$ are the Lagrange multipliers to be determined optimally using the theory of calculus of variations [64, 65], and $\tilde{\wp}_{1,n}$, $\tilde{\wp}_{2,n}$ denote restricted variations. Different Lagrange multipliers and their interpretations are provided in detail by He [63].

Finally, the exact solutions of the coupled system are obtained as

$$\wp_1(\tau,\upsilon) = \lim_{n\to\infty} \wp_{1,n}(\tau,\upsilon), \qquad \wp_2(\tau,\upsilon) = \lim_{n\to\infty} \wp_{2,n}(\tau,\upsilon). \tag{32}$$

5. Applications of the proposed methods

This section demonstrates the applicability and effectiveness of the proposed semi-analytical methods for solving nonlinear fractional coupled KdV-type systems. The developed ϕ_C-qHAM and ϕ_C-VIM are applied to selected benchmark problems, including the Kersten-Krasil'shchik KdV-mKdV system and a two-component coupled KdV model. Analytical series solutions are constructed and evaluated to illustrate convergence behavior, accuracy, and computational efficiency. Furthermore, the influence of the fractional order on the dynamical behavior of the solutions is examined through graphical analysis, highlighting the role of memory effects in nonlinear wave propagation. The results confirm the reliability and robustness of the proposed methods in handling complex nonlinear fractional systems.

5.1 *Solution via the ϕ_C-qHAM*

Problem 5.1.1

Consider the Kersten–Krasil'shchik KdV–mKdV nonlinear coupled system involving the ϕ-Caputo fractional derivative of order $0 < \delta \leq 1$:

$$\begin{aligned} &D_{\upsilon}^{\delta;\phi}\wp_1 + \frac{\partial^3\wp_1}{\partial\tau^3} - 6\wp_1\frac{\partial\wp_1}{\partial\tau} + 3\wp_2\frac{\partial^3\wp_2}{\partial\tau^3} + 3\frac{\partial\wp_2}{\partial\tau}\frac{\partial^2\wp_2}{\partial\tau^2} - 3\wp_2^2\frac{\partial\wp_1}{\partial\tau} + 6\wp_1\wp_2\frac{\partial\wp_2}{\partial\tau} = 0, \\ &D_{\upsilon}^{\delta;\phi}\wp_2 + \frac{\partial^3\wp_2}{\partial\tau^3} - 3\wp_2^2\frac{\partial\wp_2}{\partial\tau} - 3\wp_1\frac{\partial\wp_2}{\partial\tau} + 3\wp_2\frac{\partial\wp_1}{\partial\tau} = 0,\end{aligned} \tag{33}$$

where $\upsilon > 0$ is the temporal variable, and $\tau \in \mathbb{R}$ is the spatial variable.

The associated initial conditions are

$$\begin{aligned} \wp_1(\tau,0) &= c - 2c\,\mathrm{sech}^2(\sqrt{c}\tau), \\ \wp_2(\tau,0) &= 2\sqrt{c}\,\mathrm{sech}(\sqrt{c}\tau). \end{aligned} \tag{34}$$

We define the nonlinear operators $\mathcal{N}_1$ and $\mathcal{N}_2$ corresponding to system (33) as

$$\begin{aligned} \mathcal{N}_1[\wp_1,\wp_2] &= D_{\mho}^{\delta;\phi}\wp_1 + \frac{\partial^3\wp_1}{\partial\tau^3} - 6\wp_1\frac{\partial\wp_1}{\partial\tau} + 3\wp_2\frac{\partial^3\wp_2}{\partial\tau^3} + 3\frac{\partial\wp_2}{\partial\tau}\frac{\partial^2\wp_2}{\partial\tau^2} \\ &\quad - 3\wp_2^2\frac{\partial\wp_1}{\partial\tau} + 6\wp_1\wp_2\frac{\partial\wp_2}{\partial\tau}, \\ \mathcal{N}_2[\wp_1,\wp_2] &= D_{\mho}^{\delta;\phi}\wp_2 + \frac{\partial^3\wp_2}{\partial\tau^3} - 3\wp_2^2\frac{\partial\wp_2}{\partial\tau} - 3\wp_1\frac{\partial\wp_2}{\partial\tau} + 3\wp_2\frac{\partial\wp_1}{\partial\tau}. \end{aligned} \tag{35}$$

Following the ϕ-CqHAM framework, the zeroth-order deformation equations are constructed as

$$\begin{aligned} (1-qn)\mathcal{L}(\Phi_1 - \wp_{1,0}) &= hq\,\mathcal{H}(\tau,\mho)\,\mathcal{N}_1[\Phi_1,\Phi_2], \\ (1-qn)\mathcal{L}(\Phi_2 - \wp_{2,0}) &= hq\,\mathcal{H}(\tau,\mho)\,\mathcal{N}_2[\Phi_1,\Phi_2], \end{aligned} \qquad 0 \le q \le \frac{1}{n}, \tag{36}$$

where $\mathcal{L}$ denotes a suitably chosen linear operator, $h \neq 0$ is the auxiliary parameter, and $\mathcal{H}(\tau,\mho) \neq 0$ is an auxiliary function.

For $q = 0$ and $q = \frac{1}{n}$, one obtains

$$\begin{aligned} \Phi_1(\tau,\mho;0) &= \wp_{1,0}(\tau,\mho), \qquad \Phi_1\left(\tau,\mho;\frac{1}{n}\right) = \wp_1(\tau,\mho), \\ \Phi_2(\tau,\mho;0) &= \wp_{2,0}(\tau,\mho), \qquad \Phi_2\left(\tau,\mho;\frac{1}{n}\right) = \wp_2(\tau,\mho). \end{aligned} \tag{37}$$

Each embedding function admits the series expansion

$$\begin{aligned} \Phi_1(\tau,\mho;q) &= \wp_{1,0}(\tau,\mho) + \sum_{m=1}^{\infty}\wp_{1,m}(\tau,\mho)q^m, \\ \Phi_1(\tau,\mho;q) &= \wp_{2,0}(\tau,\mho) + \sum_{m=1}^{\infty}\wp_{2,m}(\tau,\mho)q^m. \end{aligned} \tag{38}$$

Differentiating the zeroth-order deformation equations m times with respect to q, setting $q=0$, and dividing by $m!$, the m^{th}-order deformation equations are obtained as

$$\begin{aligned}\mathscr{L}(\wp_{1,m}-k_m\wp_{1,m-1})&=h\mathscr{H}(\tau,\upsilon)\mathscr{R}_{1,m}(\vec{\wp}_{1,m-1},\vec{\wp}_{2,m-1}),\\ \mathscr{L}(\wp_{2,m}-k_m\wp_{2,m-1})&=h\mathscr{H}(\tau,\upsilon)\mathscr{R}_{2,m}(\vec{\wp}_{1,m-1},\vec{\wp}_{2,m-1}),\end{aligned}\tag{39}$$

where

$$k_m=\begin{cases}0, & m\le 1,\\ n, & m>1,\end{cases}$$

and $\mathscr{R}_{1,m}$ and $\mathscr{R}_{2,m}$ are the residual operators generated from $\mathscr{N}_1$ and $\mathscr{N}_2$.

Solving recursively subject to the initial conditions (34), the first-order terms are obtained as

$$\begin{aligned}\wp_{1,1}(\tau,\upsilon)&=-\frac{4c^{5/2}h(\phi(\upsilon)-\phi(\vartheta))^{\delta}\left(7\cosh(2\sqrt{c}\tau)-17\right)\tanh(\sqrt{c}\tau)\operatorname{sech}^4(\sqrt{c}\tau)}{\Gamma(\delta+1)},\\ \wp_{2,1}(\tau,\upsilon)&=\frac{2c^2h(\phi(\upsilon)-\phi(\vartheta))^{\delta}\left(\cosh(2\sqrt{c}\tau)+25\right)\tanh(\sqrt{c}\tau)\operatorname{sech}^3(\sqrt{c}\tau)}{\Gamma(\delta+1)}.\end{aligned}\tag{40}$$

The second-order components are

$$\begin{aligned}&\wp_{1,2}(\tau,\upsilon)\\ &=c^{5/2}h(\phi(\upsilon)-\phi(\vartheta))^{\delta}\operatorname{sech}^5(\sqrt{c}\tau)\left[\frac{2(n+h)\left(41\sinh(\sqrt{c}\tau)-7\sinh(3\sqrt{c}\tau)\right)}{\Gamma(\delta+1)}\right.\\ &\left.-\frac{c^{3/2}h(\phi(\upsilon)-\phi(\vartheta))^{\delta}\left(-29013\cosh(2\sqrt{c}\tau)+2112\cosh(4\sqrt{c}\tau)+13\cosh(6\sqrt{c}\tau)+32248\right)\operatorname{sech}^3(\sqrt{c}\tau)}{\Gamma(2\delta+1)}\right],\\ &\wp_{2,2}(\tau,\upsilon)\\ &=\frac{1}{4}c^2h(\phi(\upsilon)-\phi(\vartheta))^{\delta}\operatorname{sech}^4(\sqrt{c}\tau)\left[\frac{4(n+h)\left(49\sinh(\sqrt{c}\tau)+\sinh(3\sqrt{c}\tau)\right)}{\Gamma(\delta+1)}\right.\\ &\left.+\frac{c^{3/2}h(\phi(\upsilon)-\phi(\vartheta))^{\delta}\left(11119\cosh(2\sqrt{c}\tau)-146\cosh(4\sqrt{c}\tau)+\cosh(6\sqrt{c}\tau)-14078\right)\operatorname{sech}^3(\sqrt{c}\tau)}{\Gamma(2\delta+1)}\right].\end{aligned}\tag{41}$$

Hence, the ϕ_C-qHAM series solutions of system (33) are expressed as

$$\begin{aligned}\wp_1(\tau,\upsilon) &= \wp_{1,0}(\tau,\upsilon)+\sum_{m=1}^{2}\wp_{1,m}(\tau,\upsilon)\left(\frac{1}{n}\right)^m,\\ \wp_2(\tau,\upsilon) &= \wp_{2,0}(\tau,\upsilon)+\sum_{m=1}^{2}\wp_{2,m}(\tau,\upsilon)\left(\frac{1}{n}\right)^m.\end{aligned} \tag{42}$$

The higher-order terms are omitted for brevity.

$$\begin{aligned}\wp_1(\tau,\upsilon) &= c-2c\,\mathrm{sech}^2\left(\sqrt{c}\tau\right)-\frac{4c^{5/2}\hbar(\phi(\upsilon)-\phi(\vartheta))^{\delta}\left(7\cosh\left(2\sqrt{c}\tau\right)-17\right)\tanh\left(\sqrt{c}\tau\right)\mathrm{sech}^4\left(\sqrt{c}\tau\right)}{\Gamma(\delta+1)}\\ &+c^{5/2}\hbar(\phi(\upsilon)-\phi(\vartheta))^{\delta}\mathrm{sech}^5\left(\sqrt{c}\tau\right)\left[\frac{2(n+\hbar)\left(41\sinh\left(\sqrt{c}\tau\right)-7\sinh\left(3\sqrt{c}\tau\right)\right)}{\Gamma(\delta+1)}\right.\\ &\left.-\frac{c^{3/2}\hbar(\phi(\upsilon)-\phi(\vartheta))^{\delta}\left(-29013\cosh\left(2\sqrt{c}\tau\right)+2112\cosh\left(4\sqrt{c}\tau\right)+13\cosh\left(6\sqrt{c}\tau\right)+32248\right)\mathrm{sech}^3\left(\sqrt{c}\tau\right)}{\Gamma(2\delta+1)}\right],\end{aligned} \tag{43}$$

$$\begin{aligned}\wp_2(\tau,\upsilon) &= 2\sqrt{c}\,\mathrm{sech}\left(\sqrt{c}\tau\right)+\frac{2c^2\hbar(\phi(\upsilon)-\phi(\vartheta))^{\delta}\left(\cosh\left(2\sqrt{c}\tau\right)+25\right)\tanh\left(\sqrt{c}\tau\right)\mathrm{sech}^3\left(\sqrt{c}\tau\right)}{\Gamma(\delta+1)}\\ &+\frac{1}{4}c^2\hbar(\phi(\upsilon)-\phi(\vartheta))^{\delta}\mathrm{sech}^4\left(\sqrt{c}\tau\right)\left[\frac{4(n+\hbar)\left(49\sinh\left(\sqrt{c}\tau\right)+\sinh\left(3\sqrt{c}\tau\right)\right)}{\Gamma(\delta+1)}\right.\\ &\left.+\frac{c^{3/2}\hbar(\phi(\upsilon)-\phi(\vartheta))^{\delta}\left(11119\cosh\left(2\sqrt{c}\tau\right)-146\cosh\left(4\sqrt{c}\tau\right)+\cosh\left(6\sqrt{c}\tau\right)-14078\right)\mathrm{sech}^3\left(\sqrt{c}\tau\right)}{\Gamma(2\delta+1)}\right].\end{aligned}$$

For $\delta=1$, $\phi(\upsilon)=\upsilon$, $h=-1$, and $n=1$, the series solutions converge to the exact classical solutions

$$\begin{aligned}\wp_1(\tau,\upsilon) &= c-2c\,\mathrm{sech}^2\left(\sqrt{c}(2c\upsilon+\tau)\right),\\ \wp_2(\tau,\upsilon) &= 2\sqrt{c}\,\mathrm{sech}\left(\sqrt{c}(2c\upsilon+\tau)\right).\end{aligned} \tag{44}$$

The comprehensive numerical evidence presented in Tables 1–12 unequivocally establishes both the ϕ_C-qHAM and ϕ_C-VIM as powerful, accurate, and reliable tools for solving nonlinear fractional coupled KdV-type systems. The VIM method generally exhibits slightly superior accuracy, particularly for complex coupled systems with sharp gradients, while the q-HAM method offers exceptional consistency and the flexibility of convergence-control parameters. The systematic variation of fractional order reveals that lower δ values produce smoother, more diffuse wave profiles with reduced amplitudes, reflecting enhanced memory effects and energy dissipation, while higher δ values restore the sharp, localized

soliton structures characteristic of integer-order systems. The excellent agreement between both methods and the exact classical solutions at $\delta = 1$ provides rigorous validation of the theoretical framework, while the smooth transition to fractional regimes demonstrates the physical consistency of the proposed models. These findings collectively confirm that fractional-order formulations with appropriate semi-analytical solution techniques offer a versatile and physically meaningful approach for studying nonlinear wave phenomena in complex media where memory effects and nonlocal interactions play significant roles.

Table 1. Comparison of approximate solution $\wp_1(\tau,\upsilon)$ using ϕ_C-qHAM for different δ values at $\upsilon = 0.01$ and $c = 0.1$

τ	$\delta = 0.45$	$\delta = 0.65$	$\delta = 1.00$	Exact	AE ($\delta = 1$)
-10	0.00159169274286127	0.00159698976459449	0.00160001182246679	0.00160025728522961	2.4546×10^{-7}
-8	-0.00118223219422626	-0.00118165856937416	-0.00118118910671882	-0.00118140034263906	2.1124×10^{-7}
-6	-0.00422257572109670	-0.00422815588787948	-0.00423108370062828	-0.00423186097300080	7.7727×10^{-7}
-4	-0.00709744501062269	-0.00710675436031030	-0.00711192559115277	-0.00711303579699790	1.1102×10^{-6}
-2	-0.00920943303403803	-0.00921611776805426	-0.00922017344634138	-0.00922101140146566	8.3796×10^{-7}
0	-0.01000144556000355	-0.01000019366941460	-0.01000000268000000	-0.00999999999200000	2.6880×10^{-9}
2	-0.00923400302025678	-0.00922583155087465	-0.00922154905505038	-0.00922070790359940	8.4115×10^{-7}
4	-0.00712780600223767	-0.00711875683270273	-0.00711362529511111	-0.00711251563848798	1.1097×10^{-6}
6	-0.00423938556287782	-0.00423480064855357	-0.00423202467226247	-0.00423124952895413	7.7514×10^{-7}
8	-0.00117914241268824	-0.00118043665873600	-0.00118101605989291	-0.00118080636953840	2.0969×10^{-7}
10	0.00160961226338253	0.00160407390584404	0.00160101502961435	0.00160076904523633	2.4598×10^{-7}

Table 2. Comparison of approximate solution $\wp_2(\tau,\upsilon)$ using ϕ_C-qHAM for different δ values at $\upsilon = 0.01$ and $c = 0.1$

τ	$\delta = 0.45$	$\delta = 0.65$	$\delta = 1.00$	Exact	AE ($\delta = 1$)
-10	0.12982461995887620	0.12969515785222643	0.12962277983623500	0.12961282895431600	9.9509×10^{-6}
-8	0.14981458347105510	0.14964824295138449	0.14955529515576500	0.14954196964490650	1.3326×10^{-5}
-6	0.16901998396468710	0.16883234478274423	0.16872742515887068	0.16871194962420893	1.5476×10^{-5}
-4	0.18528460506223793	0.18511336921023874	0.18501733102425363	0.18500289617731885	1.4435×10^{-5}
-2	0.19623754136888025	0.19613391774932820	0.19607529687423547	0.19606637346299680	8.9234×10^{-6}
0	0.19999790717432323	0.19999971961293708	0.19999999612000000	0.19999999996000000	3.8400×10^{-9}
2	0.19589101638071377	0.19599692743853606	0.19605589728679693	0.19606482552257762	8.9282×10^{-6}
4	0.18471870558274742	0.18488965574844000	0.18498565034963880	0.18500008453234817	1.4434×10^{-5}
6	0.16840244755664280	0.16858821918011782	0.16869285388784946	0.16870832539595748	1.5472×10^{-5}
8	0.14926764721483665	0.14943202758201574	0.14952467633542005	0.14953799764299644	1.3321×10^{-5}
10	0.12939864104806184	0.12952675948151385	0.12959893250580187	0.12960888051953590	9.9480×10^{-6}

Problem 5.1.2

Consider the two-component homogeneous nonlinear coupled KdV system involving the ϕ-Caputo fractional derivative of order $0 < \delta \leq 1$:

$$\begin{aligned} &D_{\upsilon}^{\delta;\phi}\wp_1 - \frac{\partial^3 \wp_1}{\partial \tau^3} - \wp_1 \frac{\partial \wp_1}{\partial \tau} - \wp_2 \frac{\partial \wp_2}{\partial \tau} = 0, \\ &D_{\upsilon}^{\delta;\phi}\wp_2 + 2\frac{\partial^3 \wp_2}{\partial \tau^3} - \wp_1 \frac{\partial \wp_2}{\partial \tau} = 0, \qquad \upsilon > 0,\ \tau \in \mathbb{R}. \end{aligned} \tag{45}$$

The initial conditions are given by

$$\begin{aligned} \wp_1(\tau,0) &= 3-6\tanh^2\left(\frac{\tau}{2}\right), \\ \wp_2(\tau,0) &= -3\sqrt{2}c\tanh\left(\frac{\tau}{2}\right). \end{aligned} \tag{46}$$

We define the nonlinear operators associated with system (45) as

$$\begin{aligned} \mathcal{N}_1[\wp_1,\wp_2] &= D_{\mho}^{\delta;\phi}\wp_1 - \frac{\partial^3\wp_1}{\partial\tau^3} - \wp_1\frac{\partial\wp_1}{\partial\tau} - \wp_2\frac{\partial\wp_2}{\partial\tau}, \\ \mathcal{N}_2[\wp_1,\wp_2] &= D_{\mho}^{\delta;\phi}\wp_2 + 2\frac{\partial^3\wp_2}{\partial\tau^3} - \wp_1\frac{\partial\wp_2}{\partial\tau}. \end{aligned} \tag{47}$$

Following the ϕ-Caputo fractional q-homotopy analysis framework, the zeroth-order deformation equations are constructed as

$$\begin{aligned} (1-qn)\mathcal{L}(\Phi_1-\wp_{1,0}) &= hq\,\mathcal{H}(\tau,\mho)\,\mathcal{N}_1[\Phi_1,\Phi_2], \\ (1-qn)\mathcal{L}(\Phi_2-\wp_{2,0}) &= hq\,\mathcal{H}(\tau,\mho)\,\mathcal{N}_2[\Phi_1,\Phi_2], \end{aligned} \qquad 0\le q\le\frac{1}{n}, \tag{48}$$

where $\mathcal{L}$ denotes a suitable linear operator, $h\neq 0$ is the auxiliary parameter, and $\mathcal{H}(\tau,\mho)\neq 0$ is an auxiliary function.

For $q=0$ and $q=\frac{1}{n}$, one obtains

$$\begin{aligned} \Phi_1(\tau,\mho;0) &= \wp_{1,0}(\tau,\mho), \qquad \Phi_1\left(\tau,\mho;\frac{1}{n}\right) = \wp_1(\tau,\mho), \\ \Phi_2(\tau,\mho;0) &= \wp_{2,0}(\tau,\mho), \qquad \Phi_2\left(\tau,\mho;\frac{1}{n}\right) = \wp_2(\tau,\mho). \end{aligned} \tag{49}$$

Each embedding function admits the series expansion

$$\begin{aligned} \Phi_1(\tau,\mho;q) &= \wp_{1,0}(\tau,\mho) + \sum_{m=1}^{\infty}\wp_{1,m}(\tau,\mho)q^m, \\ \Phi_1(\tau,\mho;q) &= \wp_{2,0}(\tau,\mho) + \sum_{m=1}^{\infty}\wp_{2,m}(\tau,\mho)q^m. \end{aligned} \tag{50}$$

Differentiating the zeroth-order deformation equations m times with respect to q, setting $q=0$, and dividing by $m!$, the m^{th}-order deformation equations are obtained as

$$\begin{aligned}
\mathscr{L}(\wp_{1,m} - k_m \wp_{1,m-1}) &= h\mathscr{H}(\tau,\upsilon)\mathscr{R}_{1,m}(\vec{\wp}_{1,m-1}, \vec{\wp}_{2,m-1}),\\
\mathscr{L}(\wp_{2,m} - k_m \wp_{2,m-1}) &= h\mathscr{H}(\tau,\upsilon)\mathscr{R}_{2,m}(\vec{\wp}_{1,m-1}, \vec{\wp}_{2,m-1}),
\end{aligned} \tag{51}$$

where

$$k_m = \begin{cases} 0, & m \le 1,\\ n, & m > 1, \end{cases}$$

and $\mathscr{R}_{1,m}$ and $\mathscr{R}_{2,m}$ are the residual operators generated from $\mathscr{N}_1$ and $\mathscr{N}_2$.

Solving recursively and using the initial conditions (46), the first-order components are obtained as

$$\begin{aligned}
\wp_{1,1}(\tau,\upsilon) &= -\frac{3h(\phi(\upsilon)-\phi(\vartheta))^{\delta}\tanh\left(\frac{\tau}{2}\right)\operatorname{sech}^4\left(\frac{\tau}{2}\right)\left(\left(3c^2+4\right)\cosh\tau+3c^2-8\right)}{2\Gamma(\delta+1)},\\
\wp_{2,1}(\tau,\upsilon) &= -\frac{3ch(\phi(\upsilon)-\phi(\vartheta))^{\delta}(5\cosh\tau-13)\operatorname{sech}^4\left(\frac{\tau}{2}\right)}{2\sqrt{2}\Gamma(\delta+1)}.
\end{aligned} \tag{52}$$

The second-order terms are given by

$$\begin{aligned}
\wp_{1,2}(\tau,\upsilon) &= \frac{3}{32}h(\phi(\upsilon)-\phi(\vartheta))^{\delta}\operatorname{sech}^4\left(\frac{\tau}{2}\right)\left[\frac{h(\phi(\upsilon)-\phi(\vartheta))^{\delta}\operatorname{sech}^4\left(\frac{\tau}{2}\right)}{\Gamma(2\delta+1)}\Big((99c^2-456)\cosh\tau\right.\\
&\quad -48(6c^2+1)\cosh(2\tau)+(21c^2+8)\cosh(3\tau)+8(51c^2+76)\Big)-\frac{16(n+h)\tanh\left(\frac{\tau}{2}\right)}{\Gamma(\delta+1)}\\
&\quad \left.\times\Big((3c^2+4)\cosh\tau+3c^2-8\Big)\right],\\
\wp_{2,2}(\tau,\upsilon) &= 3ch(\phi(\upsilon)-\phi(\vartheta))^{\delta}\operatorname{sech}^4\left(\frac{\tau}{2}\right)\left[-\frac{(n+h)(5\cosh\tau-13)}{2\sqrt{2}\Gamma(\delta+1)}\right.\\
&\quad +\frac{h(\phi(\upsilon)-\phi(\vartheta))^{\delta}\tanh\left(\frac{\tau}{2}\right)\operatorname{sech}^2\left(\frac{\tau}{2}\right)}{8\sqrt{2}\Gamma(2\delta+1)}\Big(-4(9c^2+245)\cosh\tau-36c^2\\
&\quad \left.+25\cosh(2\tau)+2163\Big)\right].
\end{aligned} \tag{53}$$

Hence, the ϕ_C-qHAM series solutions of system (45) are expressed as

$$\begin{aligned}\wp_1(\tau,\upsilon) &= \wp_{1,0}(\tau,\upsilon)+\sum_{m=1}^{2}\wp_{1,m}(\tau,\upsilon)\left(\frac{1}{n}\right)^m,\\ \wp_2(\tau,\upsilon) &= \wp_{2,0}(\tau,\upsilon)+\sum_{m=1}^{2}\wp_{2,m}(\tau,\upsilon)\left(\frac{1}{n}\right)^m.\end{aligned} \tag{54}$$

The higher-order terms are omitted for brevity.

$$\begin{aligned}\wp_1(\tau,\upsilon) &= 3-6\tanh^2\left(\frac{\tau}{2}\right)-\frac{3\hbar(\phi(\upsilon)-\phi(\vartheta))^{\delta}\tanh\left(\frac{\tau}{2}\right)\operatorname{sech}^4\left(\frac{\tau}{2}\right)\left(\left(3c^2+4\right)\cosh(\tau)+3c^2-8\right)}{2\Gamma(\delta+1)}\\ &+\frac{3}{32}\hbar(\phi(\upsilon)-\phi(\vartheta))^{\delta}\operatorname{sech}^4\left(\frac{\tau}{2}\right)\left[\frac{\hbar(\phi(\upsilon)-\phi(\vartheta))^{\delta}\operatorname{sech}^4\left(\frac{\tau}{2}\right)}{\Gamma(2\delta+1)}\left(\left(99c^2-456\right)\cosh(\tau)\right.\right.\\ &\left.-48\left(6c^2+1\right)\cosh(2\tau)+\left(21c^2+8\right)\cosh(3\tau)+8\left(51c^2+76\right)\right)\\ &\left.-\frac{16(n+\hbar)\tanh\left(\frac{\tau}{2}\right)}{\Gamma(\delta+1)}\left(\left(3c^2+4\right)\cosh(\tau)+3c^2-8\right)\right],\end{aligned} \tag{55}$$

$$\begin{aligned}\wp_2(\tau,\upsilon) &= -3\sqrt{2}c\tanh\left(\frac{\tau}{2}\right)-\frac{3c\hbar(\phi(\upsilon)-\phi(\vartheta))^{\delta}(5\cosh(\tau)-13)\operatorname{sech}^4\left(\frac{\tau}{2}\right)}{2\sqrt{2}\Gamma(\delta+1)}\\ &+3c\hbar(\phi(\upsilon)-\phi(\vartheta))^{\delta}\operatorname{sech}^4\left(\frac{\tau}{2}\right)\left[-\frac{(n+\hbar)(5\cosh(\tau)-13)}{2\sqrt{2}\Gamma(\delta+1)}\right.\\ &\left.+\frac{\hbar(\phi(\upsilon)-\phi(\vartheta))^{\delta}\tanh\left(\frac{\tau}{2}\right)\operatorname{sech}^2\left(\frac{\tau}{2}\right)}{8\sqrt{2}\Gamma(2\delta+1)}\left(-4\left(9c^2+245\right)\cosh(\tau)-36c^2+25\cosh(2\tau)+2163\right)\right].\end{aligned}$$

For $\delta=1$, $\phi(\upsilon)=\upsilon$, $h=-1$, and $n=1$, the series solutions converge to the exact classical solutions

$$\begin{aligned}\wp_1(\tau,\upsilon) &= 3-6\tanh^2\left(\frac{\upsilon+\tau}{2}\right),\\ \wp_2(\tau,\upsilon) &= -3\sqrt{2}c\tanh\left(\frac{\upsilon+\tau}{2}\right).\end{aligned} \tag{56}$$

Table 3. Comparison of approximate solution $\wp_1(\tau,\upsilon)$ using ϕ_C-qHAM for different δ values at $\upsilon = 0.01$ and $c = 0.1$

τ	$\delta = 0.45$	$\delta = 0.65$	$\delta = 1.00$	Exact	AE ($\delta = 1$)
−10	−2.9990467800593760	−2.9989481440559453	−2.9989126766440006	−2.9989094106690910	3.2660×10^{-6}
−8	−2.9929584554272800	−2.9922316474214590	−2.9919703281458405	−2.9919462515779074	2.4077×10^{-5}
−6	−2.9480718222649540	−2.9428100606113525	−2.9409197256658812	−2.9407448443546533	1.7488×10^{-4}
−4	−2.6222724350546100	−2.5887522474102362	−2.5768250842532900	−2.5756862052745007	1.1389×10^{-3}
−2	−0.5916257993029104	−0.5058868823263691	−0.4815754059572407	−0.4782343841537089	3.3410×10^{-3}
0	3.0448808044659437	3.0023937872485470	3.0000052500000000	2.9999985000002500	6.7500×10^{-6}
2	−0.3887434706011261	−0.4554910225203498	−0.4787348413834676	−0.4820725840381308	3.3377×10^{-3}
4	−2.5185830164002683	−2.5628333032147377	−2.5753636916208755	−2.5765035175064100	1.1398×10^{-3}
6	−2.9315717235601797	−2.9386927399833580	−2.9406875986060017	−2.9408626513398843	1.7505×10^{-4}
8	−2.9906761218549747	−2.9916623293931424	−2.9919382316045806	−2.9919623321962600	2.4101×10^{-5}
10	−2.9987369861449027	−2.9988708711850074	−2.9989083202290500	−2.9989115894703815	3.2692×10^{-6}

Table 4. Comparison of approximate solution $\wp_2(\tau,\upsilon)$ using ϕ_C-qHAM for different δ values at $\upsilon = 0.01$ and $c = 0.1$

τ	$\delta = 0.45$	$\delta = 0.65$	$\delta = 1.00$	Exact	AE ($\delta = 1$)
−10	0.0424234019530160	0.0424235670783653	0.0424227424643557	0.0424225160214513	2.2644×10^{-7}
−8	0.0424043971359496	0.0424054396014009	0.0423993353083731	0.0423976655843552	1.6697×10^{-6}
−6	0.0422740364629742	0.0422723203535349	0.0422266434924326	0.0422144944892799	1.2149×10^{-5}
−4	0.0417438761822393	0.0413200369169817	0.0409650609980324	0.0408851665794830	7.9894×10^{-5}
−2	0.0377530231023005	0.0335391767788668	0.0324267144501856	0.0322222737189731	2.0444×10^{-4}
0	−0.0151570078942176	−0.0059918955027744	−0.0008485281374238	−0.0002121302666066	6.3639×10^{-4}
2	−0.0336583758718871	−0.0319936539096071	−0.0322092772289533	−0.0324004548407797	1.9118×10^{-4}
4	−0.0394408486273680	−0.0403979234157463	−0.0408342501662340	−0.0409151416325278	8.0891×10^{-5}
6	−0.0419078232300679	−0.0421272024967124	−0.0422060862205725	−0.0422186803630811	1.2594×10^{-5}
8	−0.0423537271903661	−0.0423854019337471	−0.0423964975899320	−0.0423982345110108	1.7369×10^{-6}
10	−0.0424165239142262	−0.0424208479153949	−0.0424223573940831	−0.0424225930619753	2.3567×10^{-7}

5.2 *Solution via the ϕ_C-VIM*

Problem 5.2.1

Consider the Kersten-Krasil'shchik KdV-mKdV nonlinear coupled system governed by the ϕ-Caputo fractional derivative

$$\mathscr{D}_{\upsilon}^{\delta;\phi}\wp_1(\tau,\upsilon) + \frac{\partial^3\wp_1}{\partial\tau^3} - 6\wp_1\frac{\partial\wp_1}{\partial\tau} + 3\wp_2\frac{\partial^3\wp_2}{\partial\tau^3} + 3\frac{\partial\wp_2}{\partial\tau}\frac{\partial^2\wp_2}{\partial\tau^2}$$

$$- 3\wp_2^2\frac{\partial\wp_1}{\partial\tau} + 6\wp_1\wp_2\frac{\partial\wp_2}{\partial\tau} = 0, \tag{57}$$

$$\mathscr{D}_{\upsilon}^{\delta;\phi}\wp_2(\tau,\upsilon) + \frac{\partial^3\wp_2}{\partial\tau^3} - 3\wp_2^2\frac{\partial\wp_2}{\partial\tau} - 3\wp_1\frac{\partial\wp_2}{\partial\tau} + 3\wp_2\frac{\partial\wp_1}{\partial\tau} = 0,$$

where $\upsilon > 0$ is the temporal variable, and $\tau \in \mathbb{R}$ is the spatial variable, and $0 < \delta \leq 1$.

The corresponding initial conditions are

$$\begin{aligned} \wp_1(\tau,0) &= c - 2c\,\mathrm{sech}^2\left(\sqrt{c}\,\tau\right), \\ \wp_2(\tau,0) &= 2\sqrt{c}\,\mathrm{sech}\left(\sqrt{c}\,\tau\right). \end{aligned} \tag{58}$$

Comparing system (57) with the general ϕ_C-VIM formulation, the linear and nonlinear operators are identified as

$$L_1(\wp_1,\wp_2) = \frac{\partial^3 \wp_1}{\partial \tau^3},$$

$$N_1(\wp_1,\wp_2) = -6\wp_1\frac{\partial \wp_1}{\partial \tau} + 3\wp_2\frac{\partial^3 \wp_2}{\partial \tau^3} + 3\frac{\partial \wp_2}{\partial \tau}\frac{\partial^2 \wp_2}{\partial \tau^2} - 3\wp_2^2\frac{\partial \wp_1}{\partial \tau} + 6\wp_1\wp_2\frac{\partial \wp_2}{\partial \tau},$$

$$L_2(\wp_1,\wp_2) = \frac{\partial^3 \wp_2}{\partial \tau^3},$$

$$N_2(\wp_1,\wp_2) = -3\wp_2^2\frac{\partial \wp_2}{\partial \tau} - 3\wp_1\frac{\partial \wp_2}{\partial \tau} + 3\wp_2\frac{\partial \wp_1}{\partial \tau},$$

with vanishing source terms.

According to the ϕ-Caputo fractional variational iteration method, the correction functionals are constructed as

$$\begin{aligned} \wp_{1,n+1}(\tau,\mho) &= \wp_{1,n}(\tau,\mho) - \int_0^{\mho}\left[\wp_{1,n}^{[1];\phi}(\tau,\rho) + L_1(\wp_{1,n}) + N_1(\tilde{\wp}_{1,n},\tilde{\wp}_{2,n})\right]\phi'(\rho)\,d\rho, \\ \wp_{2,n+1}(\tau,\mho) &= \wp_{2,n}(\tau,\mho) - \int_0^{\mho}\left[\wp_{2,n}^{[1];\phi}(\tau,\rho) + L_2(\wp_{2,n}) + N_2(\tilde{\wp}_{1,n},\tilde{\wp}_{2,n})\right]\phi'(\rho)\,d\rho, \end{aligned} \tag{59}$$

where the Lagrange multipliers are optimally determined as $\mu_1 = \mu_2 = -1$ (See [64, 65, 63]).

Using the initial approximations from (58) as

$$\wp_{1,0}(\tau,\mho) = c - 2c\,\mathrm{sech}^2\left(\sqrt{c}\,\tau\right), \qquad \wp_{2,0}(\tau,\mho) = 2\sqrt{c}\,\mathrm{sech}\left(\sqrt{c}\,\tau\right),$$

the first-order approximations are obtained as

$$\begin{aligned} \wp_{1,1}(\tau,\mho) &= c - 2c\,\mathrm{sech}^2\left(\sqrt{c}\,\tau\right) + \frac{4c^{5/2}(\phi(\mho)-\phi(\vartheta))^{\delta}}{\Gamma(\delta+1)}\left(7\cosh(2\sqrt{c}\tau) - 17\right)\tanh(\sqrt{c}\tau)\,\mathrm{sech}^4(\sqrt{c}\tau), \\ \wp_{2,1}(\tau,\mho) &= 2\sqrt{c}\,\mathrm{sech}(\sqrt{c}\tau) - \frac{2c^2(\phi(\mho)-\phi(\vartheta))^{\delta}}{\Gamma(\delta+1)}\left(\cosh(2\sqrt{c}\tau) + 25\right)\tanh(\sqrt{c}\tau)\,\mathrm{sech}^3(\sqrt{c}\tau). \end{aligned} \tag{60}$$

Proceeding iteratively, the second-order approximations are obtained as

$$\wp_{1,2}(\tau,\upsilon) = \frac{c}{4}\,\mathrm{sech}^8\big(\sqrt{c}\,\tau\big)\Bigg[2\cosh^6\big(\sqrt{c}\,\tau\big)\Big(\cosh\big(2\sqrt{c}\,\tau\big)-3\Big)$$

$$-\frac{4c^3(\phi(\upsilon)-\phi(\vartheta))^{2\delta}}{\Gamma(2\delta+1)}\Big(-29013\cosh\big(2\sqrt{c}\,\tau\big)+2112\cosh\big(4\sqrt{c}\,\tau\big)+13\cosh\big(6\sqrt{c}\,\tau\big)+32248\Big)$$

$$+\frac{8c^{3/2}(\phi(\upsilon)-\phi(\vartheta))^{\delta}\cosh^3(\sqrt{c}\,\tau)}{\Gamma(\delta+1)}\Big(7\sinh\big(3\sqrt{c}\,\tau\big)-41\sinh\big(\sqrt{c}\,\tau\big)\Big)$$

$$+\frac{3c^{9/2}(\phi(\upsilon)-\phi(\vartheta))^{3\delta}\Gamma(2\delta+1)\,\mathrm{sech}^3(\sqrt{c}\,\tau)}{\Gamma^2(\delta+1)\Gamma(3\delta+1)}\Big(1733854\sinh\big(\sqrt{c}\,\tau\big)-551444\sinh\big(3\sqrt{c}\,\tau\big)$$

$$+36900\sinh\big(5\sqrt{c}\,\tau\big)-233\sinh\big(7\sqrt{c}\,\tau\big)+\sinh\big(9\sqrt{c}\,\tau\big)\Big)$$

$$+\frac{48c^6(\phi(\upsilon)-\phi(\vartheta))^{4\delta}\Gamma(3\delta+1)\tanh^2(\sqrt{c}\,\tau)\,\mathrm{sech}^4(\sqrt{c}\,\tau)}{\Gamma^3(\delta+1)\Gamma(4\delta+1)}\Big(-69777\cosh\big(2\sqrt{c}\,\tau\big)$$

$$+16182\cosh\big(4\sqrt{c}\,\tau\big)+353\cosh\big(6\sqrt{c}\,\tau\big)+80282\Big)\Bigg], \tag{61}$$

$$\wp_{2,2}(\tau,\upsilon) = \frac{\sqrt{c}}{4}\,\mathrm{sech}^7\big(\sqrt{c}\,\tau\big)\Bigg[8\cosh^6\big(\sqrt{c}\,\tau\big)+\frac{c^3(\phi(\upsilon)-\phi(\vartheta))^{2\delta}}{\Gamma(2\delta+1)}\Big(11119\cosh\big(2\sqrt{c}\,\tau\big)-146\cosh\big(4\sqrt{c}\,\tau\big)$$

$$+\cosh\big(6\sqrt{c}\,\tau\big)-14078\Big)-\frac{4c^{3/2}(\phi(\upsilon)-\phi(\vartheta))^{\delta}\cosh^3(\sqrt{c}\,\tau)}{\Gamma(\delta+1)}\Big(49\sinh\big(\sqrt{c}\,\tau\big)+\sinh\big(3\sqrt{c}\,\tau\big)\Big)$$

$$+\frac{6c^6(\phi(\upsilon)-\phi(\vartheta))^{4\delta}\Gamma(3\delta+1)\,\mathrm{sech}^6(\sqrt{c}\,\tau)}{\Gamma^3(\delta+1)\Gamma(4\delta+1)}\Big(49\sinh\big(\sqrt{c}\,\tau\big)+\sinh\big(3\sqrt{c}\,\tau\big)\Big)^2$$

$$\times\Big(140\cosh\big(2\sqrt{c}\,\tau\big)+\cosh\big(4\sqrt{c}\,\tau\big)-245\Big)$$

$$-\frac{12c^{9/2}(\phi(\upsilon)-\phi(\vartheta))^{3\delta}\Gamma(2\delta+1)\,\mathrm{sech}^3(\sqrt{c}\,\tau)}{\Gamma^2(\delta+1)\Gamma(3\delta+1)}\Big(-30359\sinh\big(\sqrt{c}\,\tau\big)+6501\sinh\big(3\sqrt{c}\,\tau\big)$$

$$+\sinh\big(5\sqrt{c}\,\tau\big)+5\sinh\big(7\sqrt{c}\,\tau\big)\Big)\Bigg].$$

Hence, the ϕ_C-VIM solution of system (57) is expressed as

$$\begin{aligned} \wp_1(\tau,\upsilon) &= \wp_{1,0}(\tau,\upsilon)+\wp_{1,1}(\tau,\upsilon)+\wp_{1,2}(\tau,\upsilon)+\cdots, \\ \wp_2(\tau,\upsilon) &= \wp_{2,0}(\tau,\upsilon)+\wp_{2,1}(\tau,\upsilon)+\wp_{2,2}(\tau,\upsilon)+\cdots. \end{aligned} \tag{62}$$

For $\delta = 1$ and $\phi(\upsilon) = \upsilon$, the obtained series solutions converge to the classical exact solutions

$$\wp_1(\tau,\upsilon) = c - 2c\,\mathrm{sech}^2\left(\sqrt{c}(2c\upsilon+\tau)\right), \qquad \wp_2(\tau,\upsilon) = 2\sqrt{c}\,\mathrm{sech}\left(\sqrt{c}(2c\upsilon+\tau)\right).$$

Table 5. Comparison of approximate solution $\wp_1(\tau,\upsilon)$ using ϕ_C-VIM for different δ values at $\upsilon = 0.01$ and $c = 0.1$

τ	$\delta = 0.45$	$\delta = 0.65$	$\delta = 1.00$	Exact	AE ($\delta = 1$)
−10	0.00159169250598490	0.00159698975313937	0.00160001182244833	0.00160025728522961	2.4546×10^{-7}
−8	−0.00118223284671208	−0.00118165860093099	−0.00118118910676968	−0.00118140034263906	2.1124×10^{-7}
−6	−0.00422257649381269	−0.00422815592525123	−0.00423108370068852	−0.00423186097300080	7.7727×10^{-7}
−4	−0.00709744485106374	−0.00710675435258797	−0.00711192559114032	−0.00711303579699790	1.1102×10^{-6}
−2	−0.00920943197939185	−0.00921611771703855	−0.00922017344625914	−0.00922101140146566	8.3796×10^{-7}
0	−0.01000144556000355	−0.01000019366941460	−0.01000000268000000	−0.00999999999200000	2.6880×10^{-9}
2	−0.00923400407504209	−0.00922583160189286	−0.00922154905513262	−0.00922070790359940	8.4115×10^{-7}
4	−0.00712780616208655	−0.00711875684043027	−0.00711362529512357	−0.00711251563848798	1.1097×10^{-6}
6	−0.00423938479047668	−0.00423480061118747	−0.00423202467220223	−0.00423124952895413	7.7514×10^{-7}
8	−0.00117914176047393	−0.00118043662718404	−0.00118101605984205	−0.00118080636953840	2.0969×10^{-7}
10	0.00160961250008295 8	0.00160407391729600	0.00160101502963281	0.00160076904523633	2.4598×10^{-7}

Table 6. Comparison of approximate solution $\wp_2(\tau,\upsilon)$ using ϕ_C-VIM for different δ values at $\upsilon = 0.01$ and $c = 0.1$

τ	$\delta = 0.45$	$\delta = 0.65$	$\delta = 1.00$	Exact	AE ($\delta = 1$)
−10	0.12982461941775503	0.12969515782606808	0.12962277983619275	0.12961282895431600	9.9509×10^{-6}
−8	0.14981458282058880	0.14964824291994352	0.14955529515571434	0.14954196964490650	1.3326×10^{-5}
−6	0.16901998397020754	0.16883234478301706	0.16872742515887124	0.16871194962420893	1.5476×10^{-5}
−4	0.18528460659973803	0.18511336928457844	0.18501733102437354	0.18500289617731885	1.4435×10^{-5}
−2	0.19623754343330313	0.19613391784916000	0.19607529687439632	0.19606637346299680	8.9234×10^{-6}
0	0.19999790717432323	0.19999971961293708	0.19999999612000002	0.19999999996000000	3.8400×10^{-9}
2	0.19589101431793327	0.19599692733873364	0.19605589728663600	0.19606482552257762	8.9282×10^{-6}
4	0.18471870404720583	0.18488965567413557	0.18498565034951905	0.18500008453234817	1.4434×10^{-5}
6	0.16840244755074810	0.16858821917983846	0.16869285388784910	0.16870832539595748	1.5472×10^{-5}
8	0.14926764786383728	0.14943202761343040	0.14952467633547070	0.14953799764299644	1.3321×10^{-5}
10	0.12939864158813408	0.12952675950765322	0.12959893250584398	0.12960888051953590	9.9480×10^{-6}

Problem 5.2.2

Consider the two-component homogeneous nonlinear coupled KdV system governed by the ϕ-Caputo fractional derivative

$$\mathscr{D}_{\mho}^{\delta;\phi}\wp_1(\tau,\mho)-\frac{\partial^3\wp_1}{\partial\tau^3}-\wp_1\frac{\partial\wp_1}{\partial\tau}-\wp_2\frac{\partial\wp_2}{\partial\tau}=0,$$

$$\mathscr{D}_{\mho}^{\delta;\phi}\wp_2(\tau,\mho)+2\frac{\partial^3\wp_2}{\partial\tau^3}-\wp_1\frac{\partial\wp_2}{\partial\tau}=0,\qquad \mho>0,\ \tau\in\mathbb{R},\ 0<\delta\leq 1. \tag{63}$$

The corresponding initial conditions are

$$\wp_1(\tau,0)=3-6\tanh^2\left(\frac{\tau}{2}\right),$$

$$\wp_2(\tau,0)=-3\sqrt{2}c\tanh\left(\frac{\tau}{2}\right). \tag{64}$$

Comparing system (63) with the general ϕ_C-VIM formulation, the linear and nonlinear operators are identified as

$$L_1(\wp_1,\wp_2)=-\frac{\partial^3\wp_1}{\partial\tau^3},\quad N_1(\wp_1,\wp_2)=-\wp_1\frac{\partial\wp_1}{\partial\tau}-\wp_2\frac{\partial\wp_2}{\partial\tau},$$

$$L_2(\wp_1,\wp_2)=2\frac{\partial^3\wp_2}{\partial\tau^3},\quad N_2(\wp_1,\wp_2)=-\wp_1\frac{\partial\wp_2}{\partial\tau},$$

with vanishing source terms.

According to the ϕ-Caputo fractional variational iteration method, the correction functionals are constructed as

$$\wp_{1,n+1}(\tau,\mho)=\wp_{1,n}(\tau,\mho)+\int_0^{\mho}\mu_1(\rho)\left[\wp_{1,n}^{[1];\phi}(\tau,\rho)-\frac{\partial^3\wp_{1,n}}{\partial\tau^3}-\wp_{1,n}\frac{\partial\wp_{1,n}}{\partial\tau}-\wp_{2,n}\frac{\partial\wp_{2,n}}{\partial\tau}\right]\phi'(\rho)\,d\rho,$$

$$\wp_{2,n+1}(\tau,\mho)=\wp_{2,n}(\tau,\mho)+\int_0^{\mho}\mu_2(\rho)\left[\wp_{2,n}^{[1];\phi}(\tau,\rho)+2\frac{\partial^3\wp_{2,n}}{\partial\tau^3}-\wp_{1,n}\frac{\partial\wp_{2,n}}{\partial\tau}\right]\phi'(\rho)\,d\rho. \tag{65}$$

where the Lagrange multipliers are optimally determined as $\mu_1=\mu_2=-1$ (See [64, 65, 63]).

Using the initial approximations from (64) as

$$\wp_{1,0}(\tau,\mho)=3-6\tanh^2\left(\frac{\tau}{2}\right),\qquad \wp_{2,0}(\tau,\mho)=-3\sqrt{2}c\tanh\left(\frac{\tau}{2}\right),$$

the first-order approximations are obtained as

$$\wp_{1,1}(\tau,\upsilon) = 3 - 6\tanh^2\Big(\frac{\tau}{2}\Big) + \frac{3(\phi(\upsilon)-\phi(\vartheta))^{\delta}}{2\Gamma(\delta+1)}\tanh\Big(\frac{\tau}{2}\Big)\operatorname{sech}^4\Big(\frac{\tau}{2}\Big) \times \Big(\big(3c^2+4\big)\cosh(\tau) + 3c^2 - 8\Big),$$

$$\wp_{2,1}(\tau,(\phi(\upsilon)-\phi(\vartheta))) = -3\sqrt{2}c\tanh\Big(\frac{\tau}{2}\Big) + \frac{3c(\phi(\upsilon)-\phi(\vartheta))^{\delta}}{2\sqrt{2}\Gamma(\delta+1)}(5\cosh(\tau)-13)\operatorname{sech}^4\Big(\frac{\tau}{2}\Big). \tag{66}$$

Proceeding similarly, the second-order approximations are derived as

$$\begin{aligned}
\wp_{1,2}(\tau,\upsilon) = \frac{3}{128}\operatorname{sech}^{10}\big(\tfrac{\tau}{2}\big)\Bigg[& -64\cosh^8\big(\tfrac{\tau}{2}\big)\big(\cosh\tau - 3\big) + \frac{4(\phi(\upsilon)-\phi(\vartheta))^{2\delta}\cosh^2\big(\frac{\tau}{2}\big)}{\Gamma(2\delta+1)}\Big((99c^2-456)\cosh\tau \\
& - 48(6c^2+1)\cosh(2\tau) + (21c^2+8)\cosh(3\tau) + 8(51c^2+76)\Big) \\
& + \frac{64(\phi(\upsilon)-\phi(\vartheta))^{\delta}\sinh\big(\frac{\tau}{2}\big)\cosh^5\big(\frac{\tau}{2}\big)}{\Gamma(\delta+1)}\Big((3c^2+4)\cosh\tau + 3c^2 - 8\Big) \\
& - \frac{6(\phi(\upsilon)-\phi(\vartheta))^{3\delta}\Gamma(2\delta+1)\tanh\big(\frac{\tau}{2}\big)}{\Gamma^2(\delta+1)\Gamma(3\delta+1)}\Big(-6(137c^2+96)\cosh(2\tau) \\
& + (2c^2+1)(9c^2+32)\cosh(3\tau) + 3(-54c^4+317c^2+928)\cosh\tau - 2(72c^4-923c^2+1184)\Big)\Bigg],
\end{aligned} \tag{67}$$

$$\begin{aligned}
\wp_{2,2}(\tau,\upsilon) = \frac{3c}{8\sqrt{2}}\operatorname{sech}^4\big(\tfrac{\tau}{2}\big)\Bigg[& \frac{4(\phi(\upsilon)-\phi(\vartheta))^{\delta}\big(5\cosh\tau - 13\big)}{\Gamma(\delta+1)} - 4\sinh\tau\,(\cosh\tau+1) \\
& + \frac{(\phi(\upsilon)-\phi(\vartheta))^{2\delta}\tanh\big(\frac{\tau}{2}\big)\operatorname{sech}^2\big(\frac{\tau}{2}\big)}{\Gamma(2\delta+1)}\Big(-4(9c^2+245)\cosh\tau - 36c^2 + 25\cosh(2\tau) + 2163\Big) \\
& - \frac{6(\phi(\upsilon)-\phi(\vartheta))^{3\delta}\Gamma(2\delta+1)\tanh^2\big(\frac{\tau}{2}\big)\operatorname{sech}^4\big(\frac{\tau}{2}\big)}{\Gamma^2(\delta+1)\Gamma(3\delta+1)} \\
& \times \Big((5\cosh\tau - 31)\big((3c^2+4)\cosh\tau + 3c^2 - 8\big)\Big)\Bigg].
\end{aligned}$$

Hence, the ϕ_C-VIM solution of system (63) is expressed as

$$\begin{aligned} \wp_1(\tau,\upsilon) &= \wp_{1,0}(\tau,\upsilon)+\wp_{1,1}(\tau,\upsilon)+\wp_{1,2}(\tau,\upsilon)+\cdots, \\ \wp_2(\tau,\upsilon) &= \wp_{2,0}(\tau,\upsilon)+\wp_{2,1}(\tau,\upsilon)+\wp_{2,2}(\tau,\upsilon)+\cdots. \end{aligned} \tag{68}$$

For $\delta = 1$ and $\phi(\upsilon) = \upsilon$, the obtained series solutions converge to the classical exact solutions

$$\wp_1(\tau,\upsilon) = 3 - 6\tanh^2\left(\frac{\tau+\upsilon}{2}\right), \qquad \wp_2(\tau,\upsilon) = -3\sqrt{2}c\tanh\left(\frac{\tau+\upsilon}{2}\right).$$

Table 7. Comparison of approximate solution $\wp_1(\tau,\upsilon)$ using ϕ_C-VIM for different δ values at $\upsilon = 0.01$ and $c = 0.1$

τ	$\delta = 0.45$	$\delta = 0.65$	$\delta = 1.00$	Exact	AE ($\delta = 1$)
−10	−2.9990467813385235	−2.9989481440714867	−2.9989126766440024	−2.9989094106690910	3.2660×10^{-6}
−8	−2.9929585246607404	−2.9922316482626540	−2.9919703281459293	−2.9919462515779074	2.4077×10^{-5}
−6	−2.9480753653570940	−2.9428101036602112	−2.9409197256702626	−2.9407448443546533	1.7488×10^{-4}
−4	−2.6223895311687540	−2.5887536701374945	−2.5768250843979987	−2.5756862052745007	1.1389×10^{-3}
−2	−0.5911847184144694	−0.5058815231578855	−0.4815754054121384	−0.4782343841537089	3.3410×10^{-3}
0	3.0448808044659432	3.0023937872485470	3.0000052500000000	2.9999985000002500	6.7500×10^{-6}
2	−0.3891845514895662	−0.4554963816888326	−0.4787348419285684	−0.4820725840381308	3.3377×10^{-3}
4	−2.5184659202861190	−2.5628318804874740	−2.5753636914761615	−2.5765035175064100	1.1398×10^{-3}
6	−2.9315681804680445	−2.9386926969345040	−2.9406875986016257	−2.9408626513398843	1.7505×10^{-4}
8	−2.9906760526215200	−2.9916623285519530	−2.9919382316044976	−2.9919623321962600	2.4101×10^{-5}
10	−2.9987369848657552	−2.9988708711694656	−2.9989083202290483	−2.9989115894703815	3.2692×10^{-6}

Table 8. Comparison of approximate solution $\wp_2(\tau,\upsilon)$ using ϕ_C-VIM for different δ values at $\upsilon = 0.01$ and $c = 0.1$

τ	$\delta = 0.45$	$\delta = 0.65$	$\delta = 1.00$	Exact	AE ($\delta = 1$)
−10	0.0424234021322333	0.0424235670870341	0.0424227424643697	0.0424225160214513	2.2644×10^{-7}
−8	0.0424044068405205	0.0424054400708144	0.0423993353091298	0.0423976655843552	1.6697×10^{-6}
−6	0.0422745347831361	0.0422723444574522	0.0422266435312895	0.0422144944892799	1.2149×10^{-5}
−4	0.0417607034994946	0.0413208508600948	0.0409650623101545	0.0408851665794830	7.9894×10^{-5}
−2	0.0376475610746807	0.0335340755443818	0.0324267062267085	0.0322222737189731	2.0444×10^{-4}
0	−0.0151570078942176	−0.0059918955027744	−0.0008485281374238	−0.0002121302666066	6.3639×10^{-4}
2	−0.0337638378995069	−0.0319987551440921	−0.0322092854524304	−0.0324004548407797	1.9118×10^{-4}
4	−0.0394240213101127	−0.0403971094726332	−0.0408342488541118	−0.0409151416325278	8.0891×10^{-5}
6	−0.0419073249099061	−0.0421271783927951	−0.0422060861817156	−0.0422186803630811	1.2594×10^{-5}
8	−0.0423537174857951	−0.0423854014643336	−0.0423964975891753	−0.0423982345110108	1.7369×10^{-6}
10	−0.0424165237350090	−0.0424208479067261	−0.0424223573940691	−0.0424225930619753	2.3567×10^{-7}

Table 9. Comparison of ϕ_C-qHAM and ϕ_C-VIM solutions $\wp_1(\tau,\upsilon)$ with absolute errors for $\delta = 1$ and $c = 0.1$ of problem 1

τ	$\phi_C - qHAM_{\delta=1}$	$\phi_C - VIM_{\delta=1}$	Exact	AE $\phi_C - qHAM_{\delta=1}$	AE $\phi_C - VIM_{\delta=1}$
−10	0.00160001182244833	0.00160001182246679	0.00160025728522961	3.2675×10^{-6}	2.4546×10^{-7}
−8	−0.00118118910676968	−0.00118118910671882	−0.00118140034263906	2.5823×10^{-7}	2.1124×10^{-7}
−6	−0.00423108370068852	−0.00423108370062828	−0.00423186097300080	3.7051×10^{-6}	7.7727×10^{-7}
−4	−0.00711192559114032	−0.00711192559115277	−0.00711303579699790	6.2814×10^{-6}	1.1102×10^{-6}
−2	−0.00922017344625914	−0.00922017344634138	−0.00922101140146566	4.8936×10^{-6}	8.3796×10^{-7}
0	−0.01000000268000000	−0.01000000268000000	−0.00999999999200000	1.9368×10^{-7}	2.6880×10^{-9}
2	−0.00922154905513262	−0.00922154905505038	−0.00922070790359940	5.1236×10^{-6}	8.4115×10^{-7}
4	−0.00711362529512357	−0.00711362529511111	−0.00711251563848798	6.2412×10^{-6}	1.1097×10^{-6}
6	−0.00423202467220223	−0.00423202467226247	−0.00423124952895413	3.5511×10^{-6}	7.7514×10^{-7}
8	−0.00118101605984205	−0.00118101605989291	−0.00118080636953840	3.6971×10^{-7}	2.0969×10^{-7}
10	0.00160101502963281	0.00160101502961435	0.00160076904523633	3.3049×10^{-6}	2.4598×10^{-7}

Table 10. Comparison of ϕ_C-qHAM and ϕ_C-VIM solutions $\wp_2(\tau,\upsilon)$ with absolute errors for $\delta = 1$ and $c = 0.1$ of problem 1

τ	$\phi_C - qHAM_{\delta=1}$	$\phi_C - VIM_{\delta=1}$	Exact	AE $\phi_C - qHAM_{\delta=1}$	AE $\phi_C - VIM_{\delta=1}$
−10	0.12962277983619275	0.12962277983623500	0.12961282895431600	9.9509×10^{-6}	9.9509×10^{-6}
−8	0.14955529515571434	0.14955529515576500	0.14954196964490650	1.3326×10^{-5}	1.3326×10^{-5}
−6	0.16872742515887124	0.16872742515887068	0.16871194962420893	1.5476×10^{-5}	1.5476×10^{-5}
−4	0.18501733102437354	0.18501733102425363	0.18500289617731885	1.4435×10^{-5}	1.4435×10^{-5}
−2	0.19607529687439632	0.19607529687423547	0.19606637346299680	8.9234×10^{-6}	8.9234×10^{-6}
0	0.19999999612000002	0.19999999612000000	0.19999999996000000	3.8400×10^{-9}	3.8400×10^{-9}
2	0.19605589728663600	0.19605589728679693	0.19606482552257762	8.9282×10^{-6}	8.9282×10^{-6}
4	0.18498565034951905	0.18498565034963880	0.18500008453234817	1.4434×10^{-5}	1.4434×10^{-5}
6	0.16869285388784910	0.16869285388784946	0.16870832539595748	1.5472×10^{-5}	1.5472×10^{-5}
8	0.14952467633547070	0.14952467633542005	0.14953799764299644	1.3321×10^{-5}	1.3321×10^{-5}
10	0.12959893250584398	0.12959893250580187	0.12960888051953590	9.9480×10^{-6}	9.9480×10^{-6}

Table 11. Comparison of ϕ_C-qHAM and ϕ_C-VIM solutions $\wp_1(\tau,\upsilon)$ with absolute errors for $\delta = 1$ and $c = 0.1$ of problem 2

τ	$\phi_C - qHAM_{\delta=1}$	$\phi_C - VIM_{\delta=1}$	Exact	AE $\phi_C - qHAM_{\delta=1}$	AE $\phi_C - VIM_{\delta=1}$
−10	−2.9989126766440024	−2.9989126766440006	−2.9989094106690910	3.8733×10^{-5}	3.2660×10^{-6}
−8	−2.9919703281459293	−2.9919703281458405	−2.9919462515779074	2.8540×10^{-4}	2.4077×10^{-5}
−6	−2.9409197256702626	−2.9409197256658812	−2.9407448443546533	2.0652×10^{-3}	1.7488×10^{-4}
−4	−2.5768250843979987	−2.5768250842532900	−2.5756862052745007	1.3066×10^{-2}	1.1389×10^{-3}
−2	−0.4815754054121384	−0.4815754059572407	−0.4782343841537089	2.7652×10^{-2}	3.3410×10^{-3}
0	3.0000052500000000	3.0000052500000000	2.9999985000002500	2.3953×10^{-3}	6.7500×10^{-6}
2	−0.4787348419285684	−0.4787348413834676	−0.4820725840381308	2.6582×10^{-2}	3.3377×10^{-3}
4	−2.5753636914761615	−2.5753636916208755	−2.5765035175064100	1.3670×10^{-2}	1.1398×10^{-3}
6	−2.9406875986016257	−2.9406875986060017	−2.9408626513398843	2.1699×10^{-3}	1.7505×10^{-4}
8	−2.9919382316044976	−2.9919382316045806	−2.9919623321962600	3.0000×10^{-4}	2.4101×10^{-5}
10	−2.9989083202290483	−2.9989083202290500	−2.9989115894703815	4.0718×10^{-5}	3.2692×10^{-6}

Table 12. Comparison of ϕ_C-qHAM and ϕ_C-VIM solutions $\wp_2(\tau,\upsilon)$ with absolute errors for $\delta = 1$ and $c = 0.1$ of problem 2

τ	$\phi_C - qHAM_{\delta=1}$	$\phi_C - VIM_{\delta=1}$	Exact	AE $\phi_C - qHAM_{\delta=1}$	AE $\phi_C - VIM_{\delta=1}$
−10	0.0424227424643697	0.0424227424643557	0.0424225160214513	2.2644×10^{-7}	2.2644×10^{-7}
−8	0.0423993353091298	0.0423993353083731	0.0423976655843552	1.6697×10^{-6}	1.6697×10^{-6}
−6	0.0422266435312895	0.0422266434924326	0.0422144944892799	1.2149×10^{-5}	1.2149×10^{-5}
−4	0.0409650623101545	0.0409650609980324	0.0408851665794830	7.9896×10^{-5}	7.9894×10^{-5}
−2	0.0324267062267085	0.0324267144501856	0.0322222737189731	2.0443×10^{-4}	2.0444×10^{-4}
0	−0.0008485281374238	−0.0008485281374238	−0.0002121302666066	6.3640×10^{-4}	6.3640×10^{-4}
2	−0.0322092854524304	−0.0322092772289533	−0.0324004548407797	1.9117×10^{-4}	1.9118×10^{-4}
4	−0.0408342488541118	−0.0408342501662340	−0.0409151416325278	8.0893×10^{-5}	8.0891×10^{-5}
6	−0.0422060861817156	−0.0422060862205725	−0.0422186803630811	1.2594×10^{-5}	1.2594×10^{-5}
8	−0.0423964975891753	−0.0423964975899320	−0.0423982345110108	1.7369×10^{-6}	1.7369×10^{-6}
10	−0.0424223573940691	−0.0424223573940831	−0.0424225930619753	2.3567×10^{-7}	2.3567×10^{-7}

6. Results and discussion

This part gives a detailed discussion of the numerical and analytical findings of the nonlinear Kersten-Krasilshik coupled KdV-mKdV system as well as the two component coupled KdV system that have been solved using the ϕ_C-qHAM and the ϕ-CFVIM. The effects of the fractional order δ on the solution, the precision of the suggested methods and the physical meaning of the solutions of these equations are discussed in detail by the use of two and three-dimensional graphs.

6.1 *Effect of the fractional order on the Kersten-Krasil'shchik system*

Figures 1 and 2 depict the three-dimensional plots of the approximate solutions $\wp_1(\tau,\upsilon)$ and $\wp_2(\tau,\upsilon)$ for fractional order $\delta = 0.45,\ 0.65,\ 0.85$, and 1.0. As can be seen, the fractional order is important to the dynamics of the waves. At smaller values of the δ, we find that the surfaces of solution undergo a significant decrease in amplitude in the time direction, which demonstrates that the memory effects and hereditary effects of the fractional operator are stronger. The profiles of the waves become sharpened as the value $\delta \to 1$ and travel with more intensity, and finally converges to the classical soliton structure for $\delta = 1$.

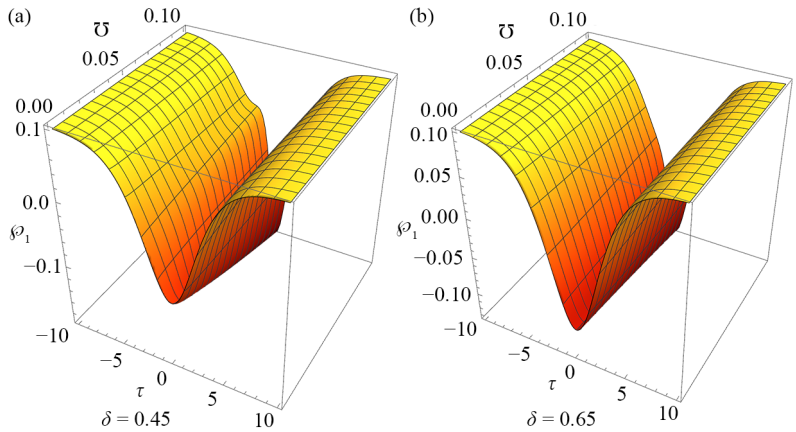


Figure 1. The effect of fractional order on the approximate solution $\wp_1(\tau,\upsilon)$ of the first and third problem in 3D for $\upsilon = 0.01$, and $c = 0.1$

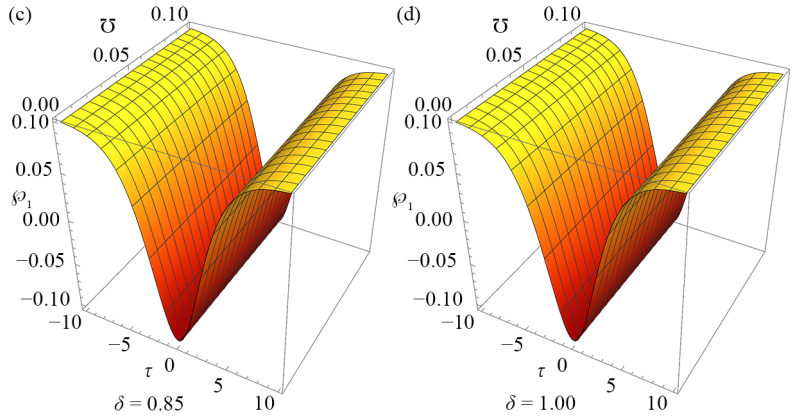


Figure 1. (cont.)

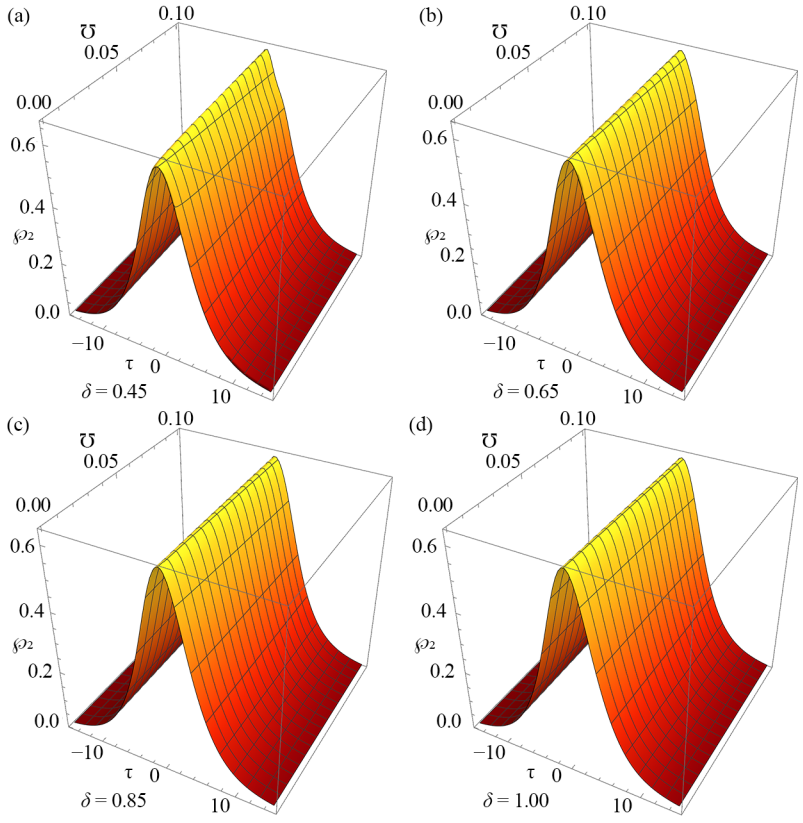


Figure 2. The effect of fractional order on the approximate solution $\wp_2(\tau, \upsilon)$ of the first and third problem in 3D for $\upsilon = 0.01$, and $c = 0.1$

This behavior is further explained by the corresponding two-dimensional plots (Figures 3 and 4). Reduction in δ results in a more diffuse and smooth wave pattern, and an increase in the fractional orders reinstates the steepness and localization of the soliton. This can be seen to indicate that the fractional derivative adds a controllable damping mechanism, which enables the model to explain intermediate physical conditions between highly dispersive and highly memory-dependent media.

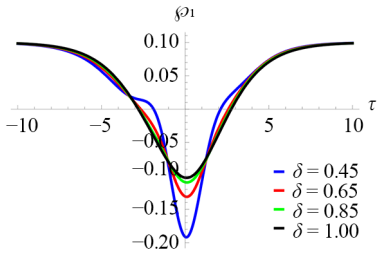


Figure 3. The effect of fractional order on the approximate solution $\wp_1(\tau,\upsilon)$ of the first and third problem in 2D for $\upsilon = 0.01$, and $c = 0.1$

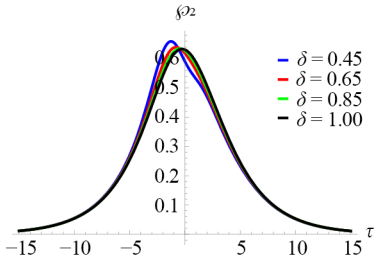


Figure 4. The effect of fractional order on the approximate solution $\wp_2(\tau,\upsilon)$ of the first and third problem in 2D for $\upsilon = 0.01$, and $c = 0.1$

6.2 *Accuracy and method comparison*

Comparisons between the exact solutions and the approximate solution obtained through ϕ_C-qHAM and ϕ_C-VIM are provided in Figures 5–8 for $\delta = 1$. The approximate solutions represented by three and two dimensional graphs are nearly identical to the exact solution, which proves the high-accuracy and convergence of both methods. The fact that the deviation in the plots is negligible proves the fact that the auxiliary parameters that are added in the formula of the ϕ_C-qHAM can effectively control the convergence and the variational correction functional also included in ϕ_C-VIM makes the formula stable and consistent.

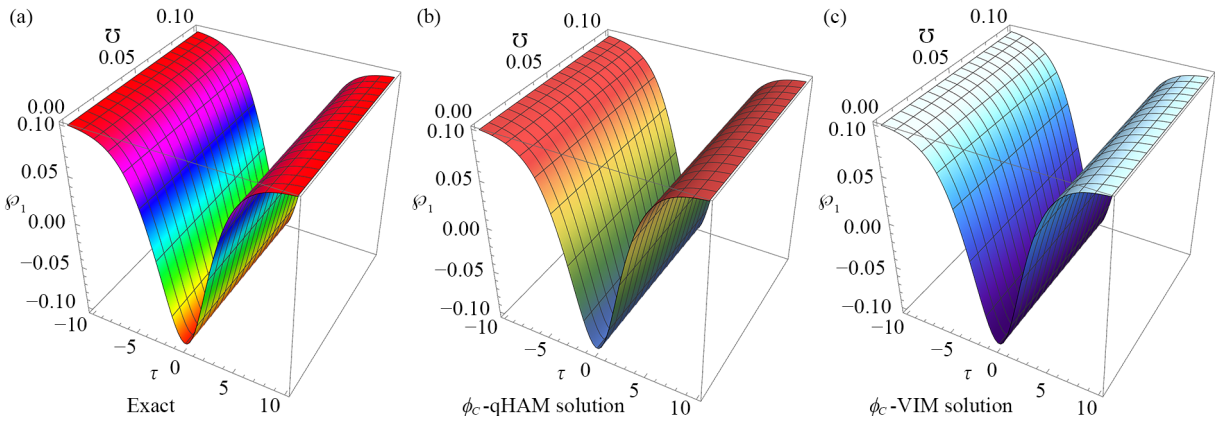


Figure 5. Comparison of the Exact solution, ϕ_C-qHAM solution, and ϕ_C-VIM solution $\wp_1(\tau,\upsilon)$ of the first and third problem for $\delta = 1$ in 3D

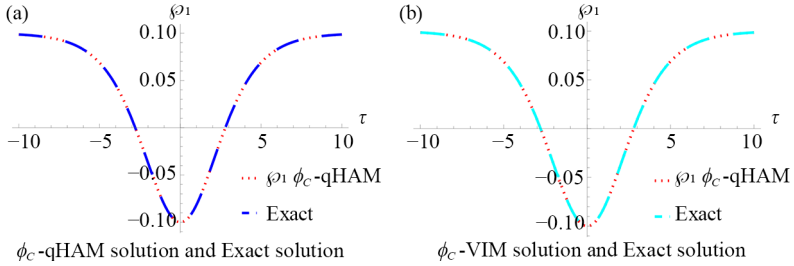


Figure 6. Comparison of the Exact solution, ϕ_C-qHAM solution, and ϕ_C-VIM solution $\wp_1(\tau,\upsilon)$ of the first and third problem for $\delta = 1$ in 2D

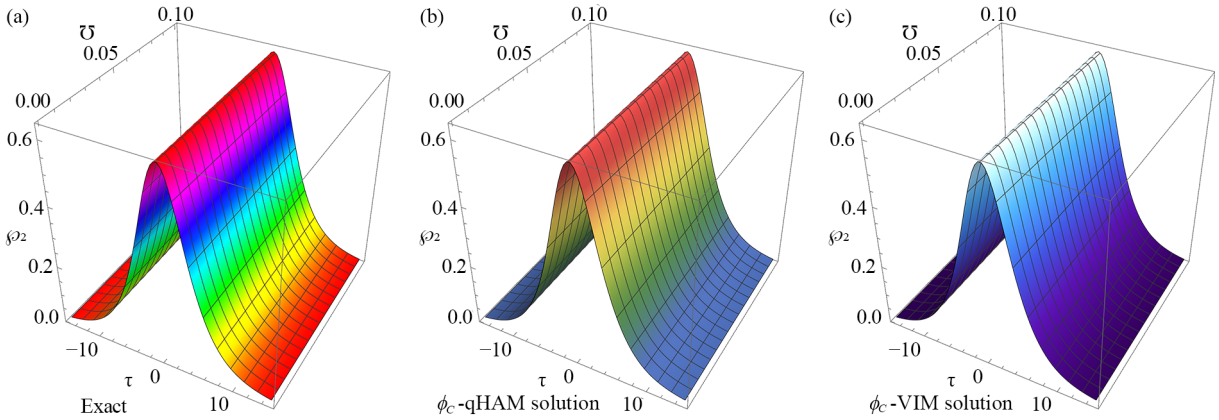


Figure 7. Comparison of the Exact solution, ϕ_C-qHAM solution, and ϕ_C-VIM solution $\wp_2(\tau,\upsilon)$ of the first and third problem for $\delta = 1$ in 3D

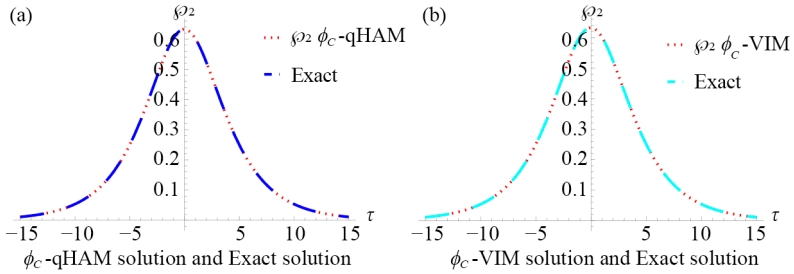


Figure 8. Comparison of the Exact solution, ϕ_C-qHAM solution, and ϕ_C-VIM solution $\wp_2(\tau,\upsilon)$ of the first and third problem for $\delta = 1$ in 2D

In addition to this, the intersecting curves in the two-dimensional plots suggest that both approaches do not violate the critical physical properties of the solutions (amplitude, symmetry and speed of waves). This validates strong capabilities of the suggested approaches of solving highly nonlinear systems of fractional order.

6.3 *Results for the two-component coupled KdV system*

Figures 9–16 show the solution of the second and fourth problem of the two-component coupled KdV system. The same tendencies can be observed with the effect of the fractional order. Figure 9 and 13 display that the smaller the value of the δ, the lower the amplitude of the oscillations and the larger the spatial area on which the wave energy is distributed. On the other hand, as δ increases a closer and narrower waveform is achieved.

As shown by the two-dimensional comparisons in Figures 12 and 16, it is evident that the solutions of the fractional-order involve a continuous family that interpolates between weakly nonlinear diffusive waves and classical integer-order

solitons. This underlines the versatility of the operator of the ϕ-Caputo in the real physical processes in which idealized integer-order assumptions cannot be adequately made.

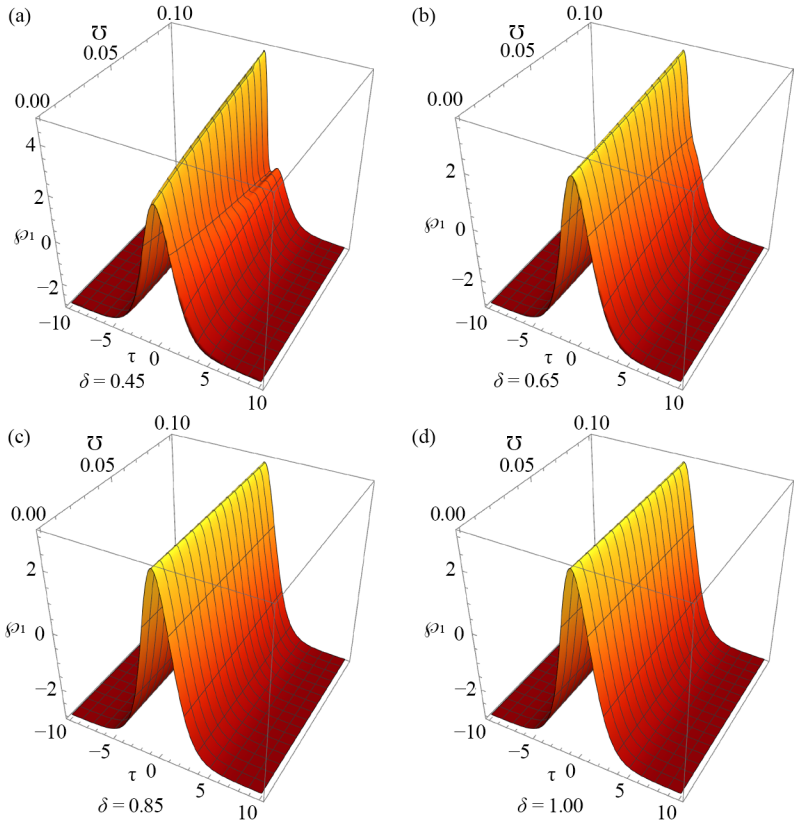


Figure 9. The effect of fractional order on the approximate solution $\wp_1(\tau, \upsilon)$ of the second and fourth problem in 3D for $\upsilon = 0.01$, and $c = 0.1$

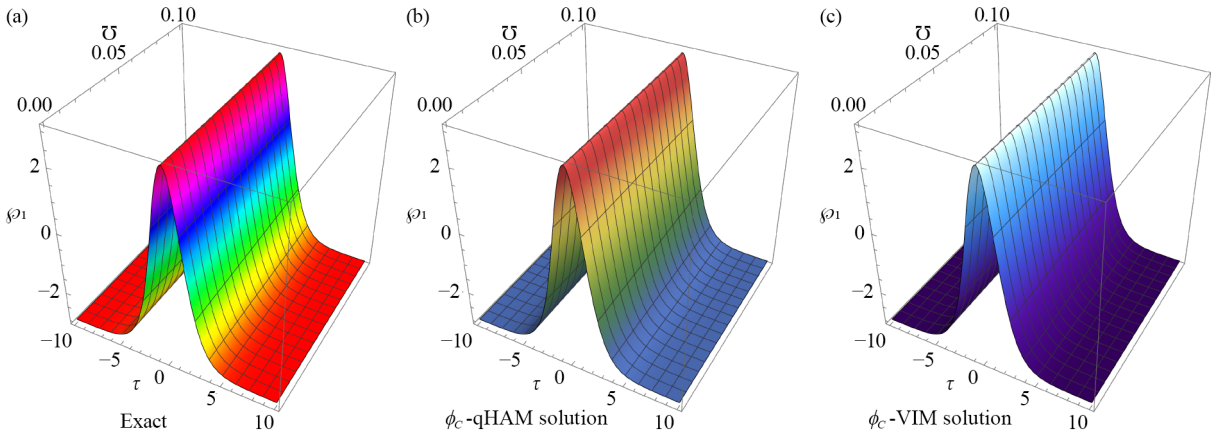


Figure 10. Comparison of the Exact solution, ϕ_C-qHAM solution, and ϕ_C-VIM solution $\wp_1(\tau, \upsilon)$ of the second and fourth problem for $\delta = 1$ in 3D

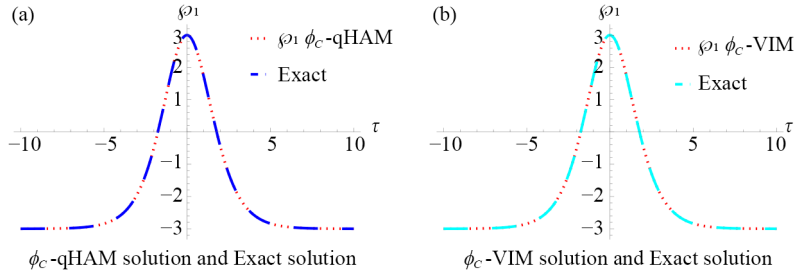


Figure 11. Comparison of the Exact solution, ϕ_C-qHAM solution, and ϕ_C-VIM solution $\wp_1(\tau,\upsilon)$ of the second and fourth problem for $\delta = 1$ in 2D

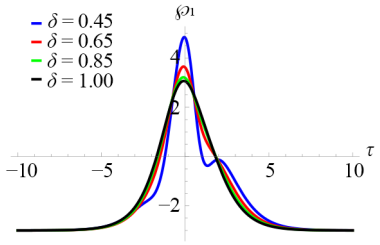


Figure 12. The effect of fractional order on the approximate solution $\wp_1(\tau,\upsilon)$ of the second and fourth problem in 2D for $\upsilon = 0.01$, and $c = 0.1$.

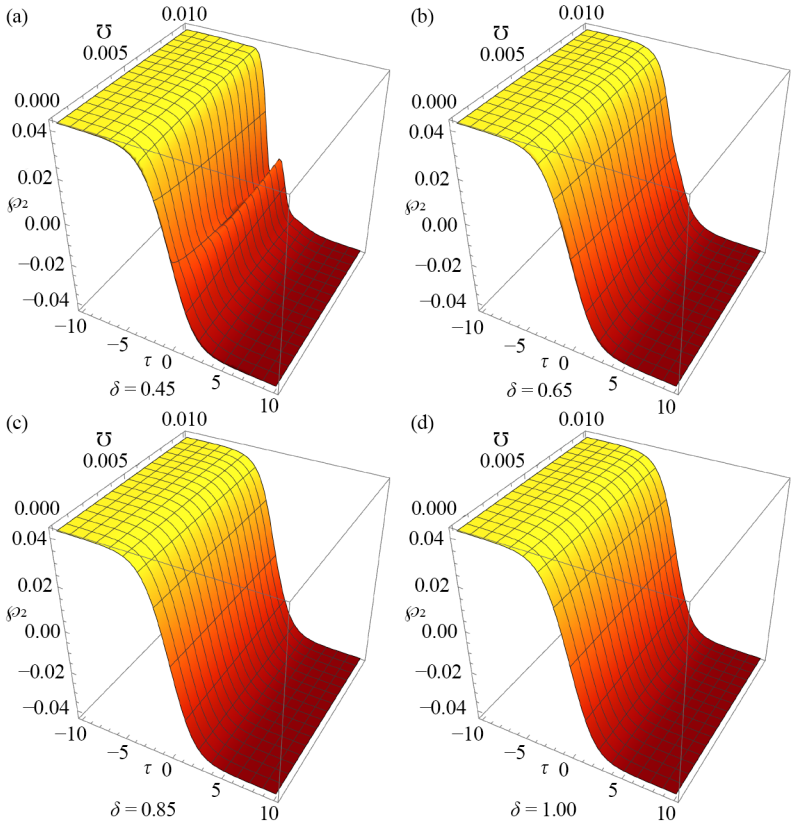


Figure 13. The effect of fractional order on the approximate solution $\wp_2(\tau,\upsilon)$ of the second and fourth problem in 3D for $\upsilon = 0.01$, and $c = 0.1$

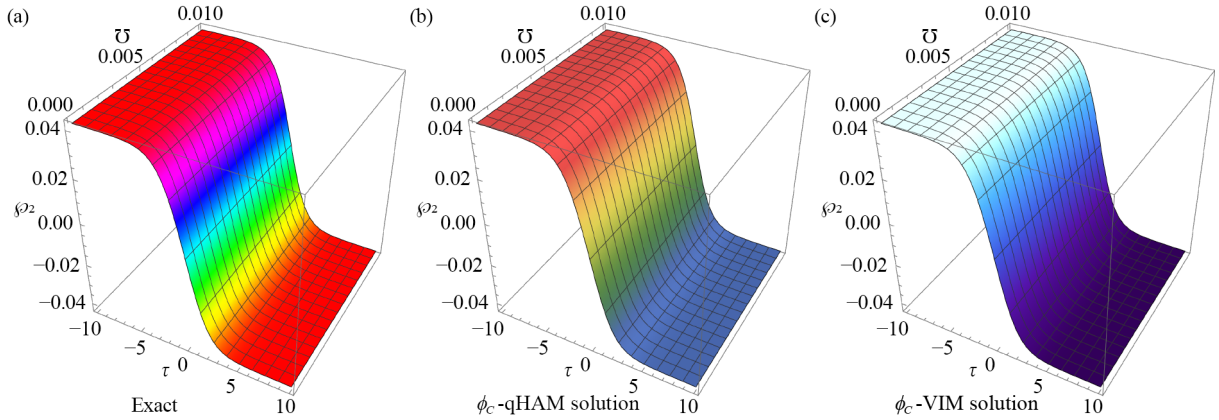


Figure 14. Comparison of the Exact solution, ϕ_C-qHAM solution, and ϕ_C-VIM solution $\wp_2(\tau,\upsilon)$ of the second and fourth problem for $\delta = 1$ in 3D

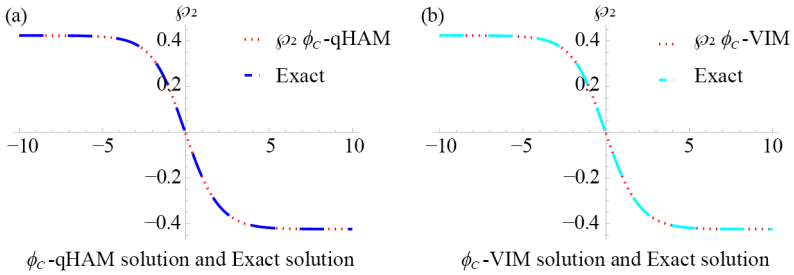


Figure 15. Comparison of the Exact solution, ϕ_C-qHAM solution, and ϕ_C-VIM solution $\wp_2(\tau,\upsilon)$ of the second and fourth problem for $\delta = 1$ in 2D

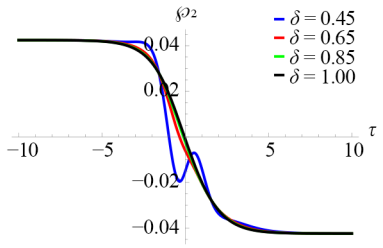


Figure 16. The effect of fractional order on the approximate solution $\wp_2(\tau,\upsilon)$ of the second and fourth problem in 2D for $\upsilon = 0.01$, and $c = 0.1$

6.4 *MAE, RMSE, relative error of the proposed models*

The statistical error analysis presented in Tables 13–16 provides a quantitative validation of the proposed methods. It is observed that the ϕ_C-VIM consistently yields lower MAE and RMSE values compared to ϕ_C-qHAM for $\wp_1$ and $\wp_2$ in both problems, indicating higher accuracy and better stability. Moreover, the relative error remains significantly small for all cases, confirming the reliability of both approaches. For $\wp_2$, both methods exhibit nearly identical performance, demonstrating their robustness. Overall, the low magnitude of MAE, RMSE, and MRE confirms the convergence and high precision of the proposed semi-analytical techniques.

Table 13. Statistical error analysis for $\wp_1(\tau,\upsilon)$ $(\delta = 1)$ of problem 1

Method	MAE	RMSE	MRE
$\phi_C - qHAM$	4.01×10^{-6}	4.52×10^{-6}	5.87×10^{-4}
$\phi_C - VIM$	7.12×10^{-7}	8.03×10^{-7}	9.61×10^{-5}

Table 14. Statistical error analysis for $\wp_2(\tau,\upsilon)$ $(\delta = 1)$ of problem 1

Method	MAE	RMSE	MRE
$\phi_C - qHAM$	1.23×10^{-5}	1.31×10^{-5}	6.12×10^{-5}
$\phi_C - VIM$	1.23×10^{-5}	1.31×10^{-5}	6.12×10^{-5}

Table 15. Statistical error analysis for $\wp_1(\tau,\upsilon)$ $(\delta = 1)$ of problem 2

Method	MAE	RMSE	MRE
$\phi_C - qHAM$	7.85×10^{-3}	1.01×10^{-2}	2.31×10^{-3}
$\phi_C - VIM$	9.42×10^{-4}	1.21×10^{-3}	2.74×10^{-4}

Table 16. Statistical error analysis for $\wp_2(\tau,\upsilon)$ $(\delta = 1)$ of problem 2

Method	MAE	RMSE	MRE
$\phi_C - qHAM$	1.28×10^{-4}	2.01×10^{-4}	3.42×10^{-3}
$\phi_C - VIM$	1.28×10^{-4}	2.01×10^{-4}	3.42×10^{-3}

6.5 *Physical significance of the models*

The Kersten-Krasil'shchik coupled KdV-mKdV system models nonlinear wave propagation phenomena in fluid dynamics, plasma physics and nonlinear lattices when the interactions between long and short waves are important. The fact that the fractional-order derivative of the ϕ-Caputo derivative is included brings the effects of memory which are inherent to complex media like viscoelastic fluids, stratified plasmas, and porous materials.

The two component coupled KdV system is that of interaction of wave modes in shallow water and nonlinear transmissions. The nonlocal time effects are reflected in the fractional formulation, which allows a more realistic expression of attenuation of waves, slow response and energy loss. The fact that the solutions are able to restore the classical soliton profiles at $\delta = 1$ proves that the proposed fractional models are physically consistent.

6.6 *Observations*

Out of all the graphical and analytical studies, it is determined that:

• Fractional order δ plays an important role in determining the amplitude of waves, the speed of propagation, and the localization of waves.

• Both the ϕ_C-qHAM and the ϕ_C-VIM produce very accurate and stably accurate approximate solutions.

• Fractional models represent a smooth flow between classical and memory-dependent dynamics.

• The proposed framework is also suitable in modeling real world nonlinear systems with hereditary effects.

Therefore, the given results confirm the usefulness of the suggested fractional methods and indicate that they have high opportunities to investigate the complicated nonlinear waves.

6.7 *Future research directions*

Several directions can be pursued in the current study to make it more effective and applicable. The potential use of the suggested ϕ_C-qHAM and the ϕ_C-VIM to more complex nonlinear equations, including the fractional Navier-Stokes equations and nonlinear Schrödinger equations, which can be found in fluid mechanics, quantum mechanics and optical wave propagation, are just one important avenue. Studying these models would give a greater insight into the contribution of memory and nonlocal effects to highly nonlinear and multi-dimensional physical processes. Moreover, future research can dwell on integrating the suggested semi-analytical methods with the current models of computation, including neural network-based solvers, to enhance the accuracy and efficiency of solutions to high-dimensional problems. The other potential direction is that there has been progress in rigorous convergence analysis and stability analysis of larger classes of fractional operators, and also in the investigation of variable-order fractional derivatives to capture more realistic time dependent memory effects. The extensions would greatly expand the focus of the existing framework and help to develop quality analytical and computational tools for the solution of complex nonlinear fractional systems.

7. Conclusion

This research has provided an analytical analysis in detail of the system of fractional order nonlinear coupled KdV-type equations using the ϕ-Caputo fractional derivative. The effectiveness and flexibility of the proposed fractional framework was shown by discussing two representative models, i.e. the Kersten-Krasil'shchik coupled KdV-mKdV system as well as two-component coupled KdV system. The memory and nonlocal time effects in the form of the ϕ-Caputo made a more realistic representation of the process of wave propagation in complex physical media. The methods of the ϕ_C-qHAM, and ϕ_C-VIM were developed and implemented to achieve the reliable approximate solutions. The validity of the obtained solutions was checked with references to the known exact solutions in the classical integer-order case, and excellent agreement was achieved, which validates the effectiveness of the offered approaches. The fractional order δ is important in determining the qualitative behavior of the solutions. The decreased fractional orders δ gave smooth profiles of the waves with lesser amplitudes, which demonstrated a greater effect in memory and energy loss, and as the increasing δ gave soliton structures that were sharper and more localized. The fact that the fractional solutions can easily be reduced to the classical soliton solutions further supports the physical consistency of the models as the model reduces to the classical soliton solutions. The findings indicate that the ϕ-Caputo fractional operator with the suggested semi-analytical methods offers a highly effective and versatile tools to study the nonlinear coupled wave systems. The given methodology can be easily generalized to other types of fractional partial differential equations that can vary in fluid mechanics, plasma physics, and other similar areas, providing avenues of future research.

Acknowledgment

The authors would like to express their sincere gratitude to the referees for their valuable comments and constructive suggestions. They also wish to acknowledge the Public Authority for Applied Education and Training (PAAET) for supporting this research under project number BE-25-08.

Author contributions

Yousuf Alkhezi, Ahmad Shafee; Conceptualization, methodology, software, validation, formal analysis, investigation, resources, data curation, writing—original draft preparation, writing—review and editing, visualization, supervision, project administration. All authors have read and agreed to the published version of the manuscript.

Data availability

The datasets used and/or analysed during the current study available from the corresponding author on reasonable request.

Conflict of interest

The authors declare no competing financial interest.

References

[1] Din A, Khan FM, Khan ZU, Yusuf A, Munir T. The mathematical study of climate change model under nonlocal fractional derivative. *Partial Differential Equations in Applied Mathematics*. 2022; 5: 100204. Available from: https://doi.org/10.1016/j.padiff.2021.100204.

[2] Jajarmi A, Baleanu D, Zarghami Vahid K, Mobayen S. A general fractional formulation and tracking control for immunogenic tumor dynamics. *Mathematical Methods in the Applied Sciences*. 2022; 45(2): 667–680. Available from: https://doi.org/10.1002/mma.7804.

[3] Modanli M, Goktepe E, Akgul A, Alsallami SA, Khalil EM. Two approximation methods for fractional order pseudo-parabolic differential equations. *Alexandria Engineering Journal*. 2022; 61(12): 10333–10339. Available from: https://doi.org/10.1016/j.aej.2022.03.061.

[4] Erturk VS, Godwe E, Baleanu D, Kumar P, Asad J, Jajarmi A. Novel fractional-order Lagrangian to describe motion of beam on nanowire. *Acta Physica Polonica A*. 2021; 140(3): 265–272. Available from: https://doi.org/10.12693/APhysPolA.140.265.

[5] Jajarmi A, Baleanu D, Vahid KZ, Pirouz HM, Asad JH. A new and general fractional Lagrangian approach: a capacitor microphone case study. *Results in Physics*. 2021; 31: 104950. Available from: https://doi.org/10.1016/j.rinp.2021.104950.

[6] Khashi'ie NS, Waini I, Zainal NA, Hamzah K, Mohd Kasim AR. Hybrid nanofluid flow past a shrinking cylinder with prescribed surface heat flux. *Symmetry*. 2020; 12(9): 1493. Available from: https://doi.org/10.3390/sym12091493.

[7] Sadek L. Introducing novel (ψ, ϕ)-fractional operators advances in fractional calculus. *Computational Methods for Differential Equations*. 2025. Available from: https://doi.org/10.22034/cmde.2025.62416.2748.

[8] Alshammari M, Alshammari TS, Alshammari S, Alsheekhhussain Z, Shah R, Jebran S, et al. Exploring new routes in fractional modeling: analytical solutions of Burgers-type systems via Caputo-Hadamard and ϕ-Caputo derivatives. *Boundary Value Problems*. 2025; 2025. Available from: https://doi.org/10.1186/s13661-025-02149-w.

[9] Ansari MSH, Malik M. Controllability of multi-term fractional-order impulsive dynamical systems with φ-Caputo fractional derivative. *Fractional Calculus and Applied Analysis*. 2025; 28: 1040–1070. Available from: https://doi.org/10.1007/s13540-025-00393-6.

[10] Sunthrayuth P, Aljahdaly NH, Ali A, Shah R, Mahariq I, Tchalla AM. Φ-Haar wavelet operational matrix method for fractional relaxation-oscillation equations containing Φ-Caputo fractional derivative. *Journal of Function Spaces*. 2021; 2021(1): 7117064. Available from: https://doi.org/10.1155/2021/7117064.

[11] Alsulami M, Alyami M, Al-Mazmumy M, Alsulami A. Semi-analytical investigation for the Ψ-Caputo fractional relaxation-oscillation equation using the decomposition method. *European Journal of Pure and Applied Mathematics*. 2024; 17(3): 2311–2398. Available from: https://doi.org/10.29020/nybg.ejpam.v17i3.5126.

[12] Singh CS, Singh H, Singh VK, Singh OP. Fractional order operational matrix methods for fractional singular integro-differential equation. *Applied Mathematical Modelling*. 2016; 40(23–24): 10705–10718. Available from: http://dx.doi.org/10.1016/j.apm.2016.08.011.

[13] Mukhtar S, Shah R, Noor S. The numerical investigation of a fractional-order multi-dimensional model of Navier-Stokes equation via novel techniques. *Symmetry*. 2022; 14(6): 1102. Available from: https://doi.org/10.3390/sym14061102.

[14] Khan H, Farooq U, Shah R, Baleanu D, Kumam P, Arif M. Analytical solutions of (2+ time fractional order) dimensional physical models, using modified decomposition method. *Applied Sciences*. 2019; 10(1): 122. Available from: https://doi.org/10.3390/app10010122.

[15] Shah R, Khan H, Baleanu D. Fractional Whitham-Broer-Kaup equations within modified analytical approaches. *Axioms*. 2019; 8(4): 125. Available from: https://doi.org/10.3390/axioms8040125.

[16] Shah R, Khan H, Kumam P, Arif M. An analytical technique to solve the system of nonlinear fractional partial differential equations. *Mathematics*. 2019; 7(6): 505. Available from: https://doi.org/10.3390/math7060505.

[17] Alaoui MK, Fayyaz R, Khan A, Shah R, Abdo MS. Analytical investigation of Noyes-field model for time fractional Belousov-Zhabotinsky reaction. *Complexity*. 2021; 2021(1): 3248376. Available from: https://doi.org/10.1155/2021/3248376.

[18] Areshi M, Khan A, Shah R, Nonlaopon K. Analytical investigation of fractional-order Newell-Whitehead-Segel equations via a novel transform. *AIMS Mathematics*. 2022; 7(4): 6936–6958. Available from: https://doi.org/10.3934/math.2022385.

[19] Kilbas AA, Srivastava HM, Trujillo JJ. *Theory and Applications of Fractional Differential Equations*. Vol. 204. Elsevier; 2006.

[20] Mainardi F. *Fractional Calculus and Waves in Linear Viscoelasticity: An Introduction to Mathematical Models*. Imperial College Press; 2010.

[21] Baleanu D, Diethelm K, Scalas E, Trujillo JJ. *Fractional Calculus: Models and Numerical Methods*. Vol. 3. World Scientific; 2012.

[22] Drazin PG, Johnson RS. *Solitons: An Introduction*. Vol. 2. Cambridge University Press; 1989.

[23] Ablowitz MJ, Segur H. *Solitons and the Inverse Scattering Transform*. Society for Industrial and Applied Mathematics; 1981. Available from: https://doi.org/10.1137/1.9781611970883.

[24] Liao S. *Beyond Perturbation: Introduction to the Homotopy Analysis Method*. Chapman and Hall/CRC; 2003. Available from: https://doi.org/10.1201/9780203491164.

[25] Osborne AR. The inverse scattering transform: tools for the nonlinear Fourier analysis and filtering of ocean surface waves. *Chaos, Solitons and Fractals*. 1995; 5(12): 2623–2637. Available from: https://doi.org/10.1016/0960-0779(94)E0118-9.

[26] Ostrovsky LA, Stepanyants YA. Do internal solitons exist in the ocean? *Reviews of Geophysics*. 1989; 27(3): 293–310. Available from: https://doi.org/10.1029/RG027i003p00293.

[27] Das GC, Sarma J. Response to "Comment on 'A new mathematical approach for finding the solitary waves in dusty plasma' [Phys. Plasmas 6, 4392 (1999)]". *Physics of Plasmas*. 1999; 6(11): 4394–4397. Available from: https://doi.org/10.1063/1.873705.

[28] Gao YT, Tian B. Ion-acoustic shocks in space and laboratory dusty plasmas: two-dimensional and non-traveling-wave observable effects. *Physics of Plasmas*. 2001; 8(7): 3146–3149. Available from: https://doi.org/10.1063/1.1379589.

[29] He JH. Approximate analytical solution for seepage flow with fractional derivatives in porous media. *Computer Methods in Applied Mechanics and Engineering*. 1998; 167(1–2): 57–68. Available from: https://doi.org/10.1016/S0045-7825(98)00108-X.

[30] Zhang J-L, Wang M-L, Wang Y-M, Fang Z-D. The improved F-expansion method and its applications. *Physics Letters A*. 2006; 350(1–2): 103–109. Available from: https://doi.org/10.1016/j.physleta.2005.10.099.

[31] Zayed EME, Zedan HA, Gepreel KA. On the solitary wave solutions for nonlinear Hirota-Satsuma coupled KdV of equations. *Chaos, Solitons and Fractals*. 2004; 22(2): 285–303. Available from: https://doi.org/10.1016/j.chaos.2003.12.045.

[32] Cao DB, Yan JR, Zhang Y. Exact solutions for a new coupled MKdV equations and a coupled KdV equations. *Physics Letters A*. 2002; 297(1–2): 68–74. Available from: https://doi.org/10.1016/S0375-9601(02)00376-6.

[33] Ganji DD, Rafei M. Solitary wave solutions for a generalized Hirota-Satsuma coupled KdV equation by homotopy perturbation method. *Physics Letters A*. 2006; 356(2): 131–137. Available from: https://doi.org/10.1016/j.physleta.2006.03.039.

[34] Hirota R, Satsuma J. Soliton solutions of a coupled Korteweg-de Vries equation. *Physics Letters A*. 1981; 85(8–9): 407–408. Available from: https://doi.org/10.1016/0375-9601(81)90423-0.

[35] Shen Y, Tian B, Zhou T-Y. In nonlinear optics, fluid dynamics and plasma physics: symbolic computation on a (2+1)-dimensional extended Calogero-Bogoyavlenskii-Schiff system. *The European Physical Journal Plus*. 2021; 136(5): 1–18. Available from: https://doi.org/10.1140/epjp/s13360-021-01323-0.

[36] Escande DF. Contributions of plasma physics to chaos and nonlinear dynamics. *Plasma Physics and Controlled Fusion*. 2016; 58(11): 113001. Available from: https://doi.org/10.1088/0741-3335/58/11/113001.

[37] Yasmin H, Aljahdaly NH, Saeed AM, Shah R. Probing families of optical soliton solutions in fractional perturbed Radhakrishnan-Kundu-Lakshmanan model with improved versions of extended direct algebraic method. *Fractal and Fractional*. 2023; 7(7): 512. Available from: https://doi.org/10.3390/fractalfract7070512.

[38] Yasmin H, Aljahdaly NH, Saeed AM, Shah R. Investigating families of soliton solutions for the complex structured coupled fractional Biswas-Arshed model in birefringent fibers using a novel analytical technique. *Fractal and Fractional*. 2023; 7(7): 491. Available from: https://doi.org/10.3390/fractalfract7070491.

[39] Liu J-G, Zhang Y-F, Wang J-J. Investigation of the time fractional generalized (2+1)-dimensional Zakharov-Kuznetsov equation with single-power law nonlinearity. *Fractals*. 2023; 31(05): 2350033. Available from: https://doi.org/10.1142/S0218348X23500330.

[40] Liu J-G, Yang X-J. Symmetry group analysis of several coupled fractional partial differential equations. *Chaos, Solitons and Fractals*. 2023; 173: 113603. Available from: https://doi.org/10.1016/j.chaos.2023.113603.

[41] Alshammari S, Al-Sawalha MM, Shah R. Approximate analytical methods for a fractional-order nonlinear system of Jaulent-Miodek equation with energy-dependent Schrödinger potential. *Fractal and Fractional*. 2023; 7(2): 140. Available from: https://doi.org/10.3390/fractalfract7020140.

[42] Alderremy AA, Shah R, Iqbal N, Aly S, Nonlaopon K. Fractional series solution construction for nonlinear fractional reaction-diffusion Brusselator model utilizing Laplace residual power series. *Symmetry*. 2022; 14(9): 1944. Available from: https://doi.org/10.3390/sym14091944.

[43] Atangana A, Secer A. The time-fractional coupled-Korteweg-de-Vries equations. *Abstract and Applied Analysis*. 2013; 2013(1): 947986. Available from: https://doi.org/10.1155/2013/947986.

[44] Akinyemi L, Iyiola OS. A reliable technique to study nonlinear time-fractional coupled Korteweg-de Vries equations. *Advances in Difference Equations*. 2020; 2020. Available from: https://doi.org/10.1186/s13662-020-02625-w.

[45] Albalawi KS, Alazman I, Prasad JG, Goswami P. Analytical solution of the local fractional KdV equation. *Mathematics*. 2023; 11(4): 882. Available from: https://doi.org/10.3390/math11040882.

[46] Li H, Peng R, Wang Z-A. On a diffusive susceptible-infected-susceptible epidemic model with mass action mechanism and birth-death effect: analysis, simulations, and comparison with other mechanisms. *SIAM Journal on Applied Mathematics*. 2018; 78(4): 2129–2153. Available from: https://doi.org/10.1137/18M1167863.

[47] Jin H-Y, Wang Z-A. Boundedness, blowup and critical mass phenomenon in competing chemotaxis. *Journal of Differential Equations*. 2016; 260(1): 162–196. Available from: https://doi.org/10.1016/j.jde.2015.08.040.

[48] He H, Peng J, Li H. Iterative approximation of fixed point problems and variational inequality problems on Hadamard manifolds. *UPB Bulletin of Science, Series A*. 2022; 84(1): 25–36.

[49] He H, Peng J, Li H. Implicit viscosity iterative algorithm for nonexpansive mapping on Hadamard manifolds. *Fixed Point Theory*. 2023; 24(1): 213-220. Available from: https://doi.org/10.24193/fpt-ro.2023.1.10.

[50] Chen H-X, Chen W, Liu X, Liu X-H. Establishing the first hidden-charm pentaquark with strangeness. *The European Physical Journal C*. 2021; 81(5): 409. Available from: https://doi.org/10.1140/epjc/s10052-021-09196-4.

[51] Lyu X, Wang X, Qi C, Sun R. Characteristics of cavity dynamics, forces, and trajectories on vertical water entries with two spheres side-by-side. *Physics of Fluids*. 2023; 35(9). Available from: https://doi.org/10.1063/5.0166794.

[52] Ayman-Mursaleen M. Approximation and convergence analysis of blending-type q-Baskakov operators using wavelet transformations. *Filomat*. 2025; 39(31): 11117–11132.

[53] Ayman-Mursaleen M. Quadratic function preserving wavelet type Baskakov operators for enhanced function approximation. *Computational and Applied Mathematics*. 2025; 44(8): 395. Available from: https://doi.org/10.1007/s40314-025-03357-x.

[54] Bhat AA, Khan A. Boundary interpolation on triangles via neural network operators. *Mathematics and Computers in Simulation*. 2025; 241: 190-201. Available from: https://doi.org/10.1016/j.matcom.2025.08.026

[55] Ayman-Mursaleen M, Lamichhane BP, Kiliçman A, Senu N. On ϑ-statistical approximation of wavelets aided Kantorovich ϑ-Baskakov operators. *Filomat*. 2024; 38(9): 3261–3274. Available from: https://doi.org/10.2298/FIL2409261A.

[56] Ayman-Mursaleen M, Saeed ST, Almohammadi SM, Arif K, Imran M. A deep neural network model for heat transfer in Darcy-Forchheimer hybrid nanofluid flow with activation energy. *Scientific Reports*. 2026. Available from: https://doi.org/10.1038/s41598-026-39536-x.

[57] Alqahtani AM, Mihoubi H, Arioua Y, Bouderah B. Analytical solutions of time-fractional Navier-Stokes equations employing homotopy perturbation-Laplace transform method. *Fractal and Fractional*. 2024; 9(1): 23. Available from: https://doi.org/10.3390/fractalfract9010023.

[58] Almeida R. A Caputo fractional derivative of a function with respect to another function. *Communications in Nonlinear Science and Numerical Simulation*. 2017; 44: 460–481. Available from: https://doi.org/10.1016/j.cnsns.2016.09.006.

[59] Samko SG, Kilbas AA, Marichev OI. *Fractional Integrals and Derivatives: Theory and Applications*. Gordon and Breach Science Publishers; 1993.

[60] Gambo YY, Jarad F, Baleanu D, Abdeljawad T. On Caputo modification of the Hadamard fractional derivatives. *Advances in Difference Equations*. 2014; 2014(1): 10. Available from: https://doi.org/10.1186/1687-1847-2014-10.

[61] Iyiola OS, Soh ME, Enyi CD. Generalised homotopy analysis method (q-HAM) for solving foam drainage equation of time fractional type. *Mathematics in Engineering, Science and Aerospace (MESA)*. 2013; 4(4): 429–440.

[62] Liao S, Tan Y. A general approach to obtain series solutions of nonlinear differential equations. *Studies in Applied Mathematics*. 2007; 119(4): 297–354. Available from: https://doi.org/10.1111/j.1467-9590.2007.00387.x.

[63] He J-H. Variational iteration method: some recent results and new interpretations. *Journal of Computational and Applied Mathematics*. 2007; 207(1): 3–17. Available from: https://doi.org/10.1016/j.cam.2006.07.009.

[64] He J-H. An alternative approach to establishment of a variational principle for the torsional problem of piezoelastic beams. *Applied Mathematics Letters*. 2016; 52: 1–3. Available from: https://doi.org/10.1016/j.aml.2015.08.001.

[65] He J-H. Generalized equilibrium equations for shell derived from a generalized variational principle. *Applied Mathematics Letters*. 2017; 64: 94–100. Available from: https://doi.org/10.1016/j.aml.2016.08.008.